PLOS | NEGLECTED TROPICAL DISEASES

RESEARCH ARTICLE

Mapping the S1 and S1' subsites of cysteine proteases with new dipeptidyl nitrile inhibitors as trypanocidal agents

Lorenzo Cianni[1,2,3,4], Carina Lemke[2], Erik Gilberg[2,3], Christian Feldmann[3], Fabiana Rosini[1], Fernanda dos Reis Rocho[1], Jean F. R. Ribeiro[1], Daiane Y. Tezuka[1,5], Carla D. Lopes[6], Sérgio de Albuquerque[6], Jürgen Bajorath[3], Stefan Laufer[4], Andrei Leitão[1], Michael Gütschow[2]*, Carlos A. Montanari[1]*

1 Medicinal Chemistry Group, Institute of Chemistry of São Carlos, University of São Paulo, São Carlos, São Paulo, Brazil, **2** Pharmaceutical Institute, Pharmaceutical Chemistry I, University of Bonn, Bonn, Germany, **3** Department of Life Science Informatics, B-IT, LIMES Program Unit Chemical Biology and Medicinal Chemistry, Rheinische Friedrich-Wilhelms-Universität, Bonn, Germany, **4** Department of Pharmaceutical/ Medicinal Chemistry, Eberhard Karls University Tübingen, Tübingen, Germany, **5** Ribeirão Preto School of Pharmaceutical Sciences, University of São Paulo, Ribeirão Preto, São Paulo, Brazil, **6** Department of Clinical Toxicological and Bromatological Analysis School of Pharmaceutical Sciences of Ribeirão Preto, University of São Paulo (USP), Ribeirão Preto, São Paulo, Brazil

* guetschow@uni-bonn.de (MG); carlos.montanari@usp.br (CAM)

Citation: Cianni L, Lemke C, Gilberg E, Feldmann C, Rosini F, Rocho FdR, et al. (2020) Mapping the S1 and S1' subsites of cysteine proteases with new dipeptidyl nitrile inhibitors as trypanocidal agents. PLoS Negl Trop Dis 14(3): e0007755. https://doi.org/10.1371/journal.pntd.0007755

Editor: Igor C. Almeida, University of Texas at El Paso, UNITED STATES

Received: August 29, 2019

Accepted: January 30, 2020

Published: March 12, 2020

Data Availability Statement: All relevant data are within the manuscript and its Supporting Information files.

Funding: We are indebted to Fundação de Amparo à Pesquisa do Estado de São Paulo – FAPESP (grant #2013/18009-4, grant #2016/07946-5 and grant #2017/17386-0) for financing this project. We also want to acknowledge the National Council for Scientific and Technological Development (CNPq, grant # 304030/2018-0) in Brazil for scholarships. We would also like to thank the

Abstract

The cysteine protease cruzipain is considered to be a validated target for therapeutic intervention in the treatment of Chagas disease. A series of 26 new compounds were designed, synthesized, and tested against the recombinant cruzain (Cz) to map its S1/S1´ subsites. The same series was evaluated on a panel of four human cysteine proteases (CatB, CatK, CatL, CatS) and *Leishmania mexicana* CPB, which is a potential target for the treatment of cutaneous leishmaniasis. The synthesized compounds are dipeptidyl nitriles designed based on the most promising combinations of different moieties in P1 (ten), P2 (six), and P3 (four different building blocks). Eight compounds exhibited a K_i smaller than 20.0 nM for Cz, whereas three compounds met these criteria for LmCPB. Three inhibitors had an EC_{50} value of ca. 4.0 μM, thus being equipotent to benznidazole according to the antitrypanosomal effects. Our mapping approach and the respective structure-activity relationships provide insights into the specific ligand-target interactions for therapeutically relevant cysteine proteases.

Author summary

Despite many achievements in identifying novel agents for the treatment of tropical and neglected diseases, further research continues to be of fundamental importance. Our research groups have been using the cruzipain cysteine protease in its recombinant form, cruzain (Cz), to identify new trypanocidal agents. Considering the possible interchangeability with other cysteine proteases, the same series of dipeptidyl nitriles was tested in *Leishmania mexicana* LmCPB. Other potential targets for such inhibitors are human

CAPES Drug Discovery program (Process #139/2015) that allowed us to evaluate LmCPB inhibitors. The funders had no role in study design, data collection and analysis, decision to publish, or preparation of the manuscript.

Competing interests: The authors have declared that no competing interests exist.

cysteine cathepsins, which are involved in different disease states. Thus, the inhibitors were also tested against cathepsins B, L, K, and S. Our results demonstrate that appropriate structural modifications of dipeptidyl nitriles can lead to inhibition of these cysteine proteases. It was also possible to identify trypanocidal agents, equipotent to benznidazole, the current drug of choice used for the treatment of Chagas disease.

Introduction

Chagas disease, aka American trypanosomiasis, is a severe health and social problem in Latin America and in new non-endemic areas such as Japan, East Europe, and the USA. Chagas disease has an annual incidence of 30,000 new cases and 10,000 deaths per year. An estimated 8 million people are infected with Chagas disease worldwide and more than 25 million people risk acquiring the disease [1].

The etiological agent, the protozoa parasite *Trypanosoma cruzi* (*T*. *cruzi*), is transmitted by blood-sucking reduviid bugs of the subfamily Triatominae [2]. The only two existing drugs in the market, benznidazole and nifurtimox, show strong side effects and inefficiency in the chronic stage of the disease [3,4]. New safe and efficacious drugs are therefore required to address with these still unmet medical needs. Initiatives such as the one launched by the Drugs for Neglected Diseases (DNDi) have led to worldwide collaborative efforts to discover new therapeutic targets [5]. Cruzain (Cz), a recombinant form of the enzyme cruzipain (EC 3.4.22.51) [6], is the most abundant cysteine protease (CP) present in the parasite and essential for its development and survival inside and outside the host cell in all forms of its life cycle. This makes Cz a druggable target for the development of new chemotherapeutic agents against Chagas disease [7,8].

Cz represents a target for irreversible (or suicide) and reversible inhibitors. K777 was at the forefront of the first generation of irreversible Cz inhibitors and initially characterized by the Sandler Center for Research in Tropical Parasitic Disease (University of California, San Francisco) [9]. Despite its ability to rescue mice of a lethal experimental *T*. *cruzi* infection and reduce parasite growth in dogs, preclinical safety and toxicology studies revealed substantial side effects of K777 in primates and dogs, even when administered in low doses [10,11]. Current research is being focused on reversible Cz inhibitors, as these are assumed to overcome possible off-target effects [12]. Drug repurposing programs of different pharmaceutical companies have recently put forward reversible inhibitors of Cz as potential drug candidates [13]. Two key compounds, Cz007 and Cz008, exhibited antiparasitic behavior in the low micromolar range for the amastigote form of the parasite and they were capable of curing *T*. *cruzi* acute form infection in an *in vivo* model. Both compounds were orally active, well-tolerated and worked most effectively at doses of 3 mg/kg [13].

The structure of Cz is closely related to those of mammalian CPs (CatL, CatK and CatS). Three-dimensional (3D) Cz structures with a variety of ligands have already been resolved [14]. The target-based molecular design was applied to generate the first series of dipeptidyl nitrile ligands as reversible Cz inhibitors with trypanocidal activity [14]. In previous work, some of us reported on low micro-molar inhibitors of Cz as modest trypanocidal agents for the amastigotes form of the *T*. *cruzi* Tulahuen strain (pEC_{50} around 4). For the most potent anti-parasite inhibitor with an EC_{50} value of 28 μM, the activity was not attributed to the general cytotoxicity of the compound [14]. More recently, the feasibility of achieving a higher Cz affinity by benefiting from the S3 structural singularity was underlined [15].

In this study, we designed a new, structurally expanded series of 26 Cz-inhibiting dipeptidyl nitriles, in particular by leveraging the P1-S1/S1'interactions. We explored the structure-activity relationships (SARs), mapped the active site of the target enzyme and evaluated the antichagasic properties of the compounds. Besides that, we have tested them against four human cysteine cathepsins (CatB, CatL, CatK, CatS) all of which constituting important targets for human diseases [16], and against the cysteine protease LmCPB, a novel macromolecular target to fight *Leishmania mexicana*. As a result of this study, several new low-nanomolar inhibitors of different CPs were discovered and three new anti-*T*. *cruzi* agents, equipotent to benznidazole, were characterized.

Methods

Modeling

Putative binding modes of novel dipeptidyl nitrile inhibitors compounds were derived from the crystal structure of *N*-(2-aminoethyl)-alpha-benzoyl-l-phenylalaninamide (33L) bound to Cz (PDB ID: 4QH6). This ligand-target-complex served as a template for knowledge-based modeling and was preprocessed using the "Structure Preparation" and "Protonate3D"-tools of the modeling software "Molecular Operating Environment" (MOE) [17], version 2018.0101, with default settings. By modification of moieties, the cocrystallized ligand was structurally transformed into the compound of interest. Obtained conformations were optimized using the force field "Amber10:EHT".

Synthetic chemistry

General considerations. The synthesis was performed as summarized in Figs 1 and 2. Melting points were determined on a Büchi 510 oil bath apparatus and are uncorrected. Infrared spectra were obtained from FT-IR Thermo Scientific Nicolet 380. Reagents, starting materials and solvents were of commercial quality and were used without further purification unless otherwise stated. All syntheses were started with enantiopure amino acids. TLC analysis was carried out on Merck 60 F_{254} silica gel plates and visualized under UV light at 254 nm and 365 nm or by using a ninhydrin staining solution. Preparative column chromatography was carried out on Grace Davison Davisil LC60A 20–45 micron or Merck Geduran Si60 63–200 micron silica using the Interchim PuriFlash 430 automated flash chromatography system. The purity of all tested compounds was determined with one of the three protocols (A-C) noted below.

A). Purity was determined via RP-HPLC on a Hewlett Packard 1090 Series II LC with a Phenomenex Luna C18 column (150 x 4.6 mm, 5 μm) and detection was performed by a UV DAD (200–440 nm). Elution was carried out with the following gradient: 0.01 M KH_2PO_4, pH 2.30 (solvent A), MeOH (solvent B), 40% B to 85% B in 8 min, 85% B for 5 min, 85% to 40% B in 1 min, 40% B for 2 min, stop time 16 min, flow 1.5 mL/min.

B). Purity was determined using an LC-MS instrument (ABSCIEX API 2000 LC-MS/MS, HPLC Agilent 1100) with a Phenomenex Luna C18 HPLC column (50 x 2.00 mm, 3 μm) and detection was performed by a UV DAD (200–440 nm). Elution was carried out with the following gradient: 0.02 M $NH_4CH_3CO_2$, pH 7.0 (solvent A), MeOH (solvent B) start with 100%, 10% B in 20 min to 100% B, 10 min 100% B, stop time 20 min, flow 0.25 mL/min.

C). Purity was determined with an LC-MS instrument (AmaZon SL ESI-MS, Shimadzu LC) with a cellulose-2 Phenomenex column (250 x 4.6 mm, 5 μm) or a Diacel column (IC-chiralpak, 250 x 4.6 mm, 5 μm). Isocratic elution with MeCN and water was applied as specified, stop time 60 min, flow 0.5 mL/min.

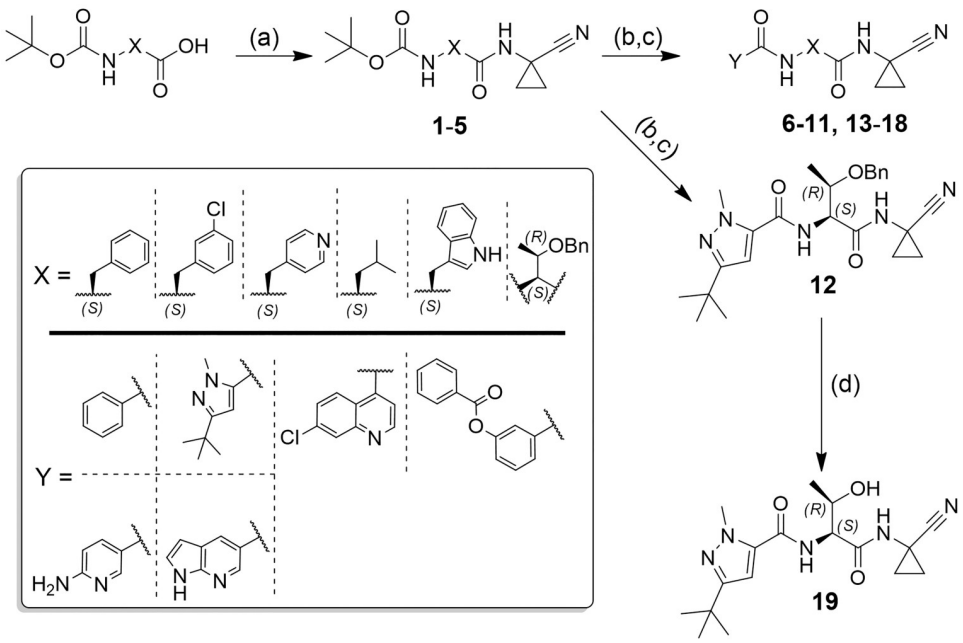

Fig 1. General synthesis of compounds 6–19. Reagents and conditions: a) HATU, DIPEA, 1-amino-1-cyclopropanecarbonitrile, DMF, rt, 18 h; b) formic acid, rt, 18 h; c) HATU or TBTU, DIPEA, carboxylic acid, DMF, rt, 18 h; d) DDQ, CH_2Cl_2, rt, 3–5 days.

https://doi.org/10.1371/journal.pntd.0007755.g001

NMR spectra were recorded on Bruker Avance 200 MHz, Bruker Avance 400 MHz, and Bruker Avance DRX 500 MHz NMR spectrometers. Chemical shifts are reported in ppm relative to TMS or the residual proton peak of the re-protonated deuterated solvent, and the spectra were calibrated against the residual proton peak of the used deuterated solvent. The following symbols indicate spin multiplicities: s (singlet), s br (broad singlet), d (doublet), dd (doublet of doublet), t (triplet), tt (triplet of triplet), q (quartet), sept (septet), and m (multiplet). Standard mass spectra were obtained either as ESI-MS (pos. and/or neg. mode) from a Advion DCMS interface, (settings as follows: ESI voltage 3.50 kV, capillary voltage 187 V, source voltage 44 V, capillary temperature 250 ˚C, desolvation gas temperature 250 ˚C, gas flow 5 L/min) or by an API 2000 mass spectrometer (electron spray ion source, ABSCIEX, Darmstadt, Germany) coupled to an Agilent 1100 HPLC system.

HRMS spectra were recorded on a Bruker micrOTOF-Q mass spectrometer connected to a Thermo Scientific Dionex UltiMate 3000 LC via an ESI interface using a Nucleodur C18 Gravity column (50 × 2.0 mm, 3 μm) or were recorded on Thermo Scientific LTQ Velos Orbitrap, in electrospray ionization (ESI) mode by direct injection.

The synthetic route was developed to optimize the set of substituents to be placed in P1, P2, and P3 that have been defined after the planning and design studies. Due to the diversity of building blocks, it was necessary to evaluate different coupling and dehydrating reagents, aiming at the best yield and preventing racemization.

General procedure for amide synthesis. **Method A**: Isobutyl chloroformate (790 mg, 0.75 mL, 5.5 mmol, 1.1 equiv) was added dropwise to a solution of Boc-(*R* or *S*) amino acid (5.0 mmol, 1.0 equiv.), DIPEA (1.6 g, 2.28 mL, 13.0 mmol, 2.6 equiv.) in dry DMF (20 mL), under argon atmosphere, at -30 ˚C and it was stirred for 0.5 h. Then, an aqueous 2 M NH_4Cl solution (294 mg, 2.75 mL, 5.50 mmol, 1.1 equiv.) was added. The resulting solution was stirred at room temperature for 20 h. The reaction mixture was dried under reduced pressure. Ethyl acetate

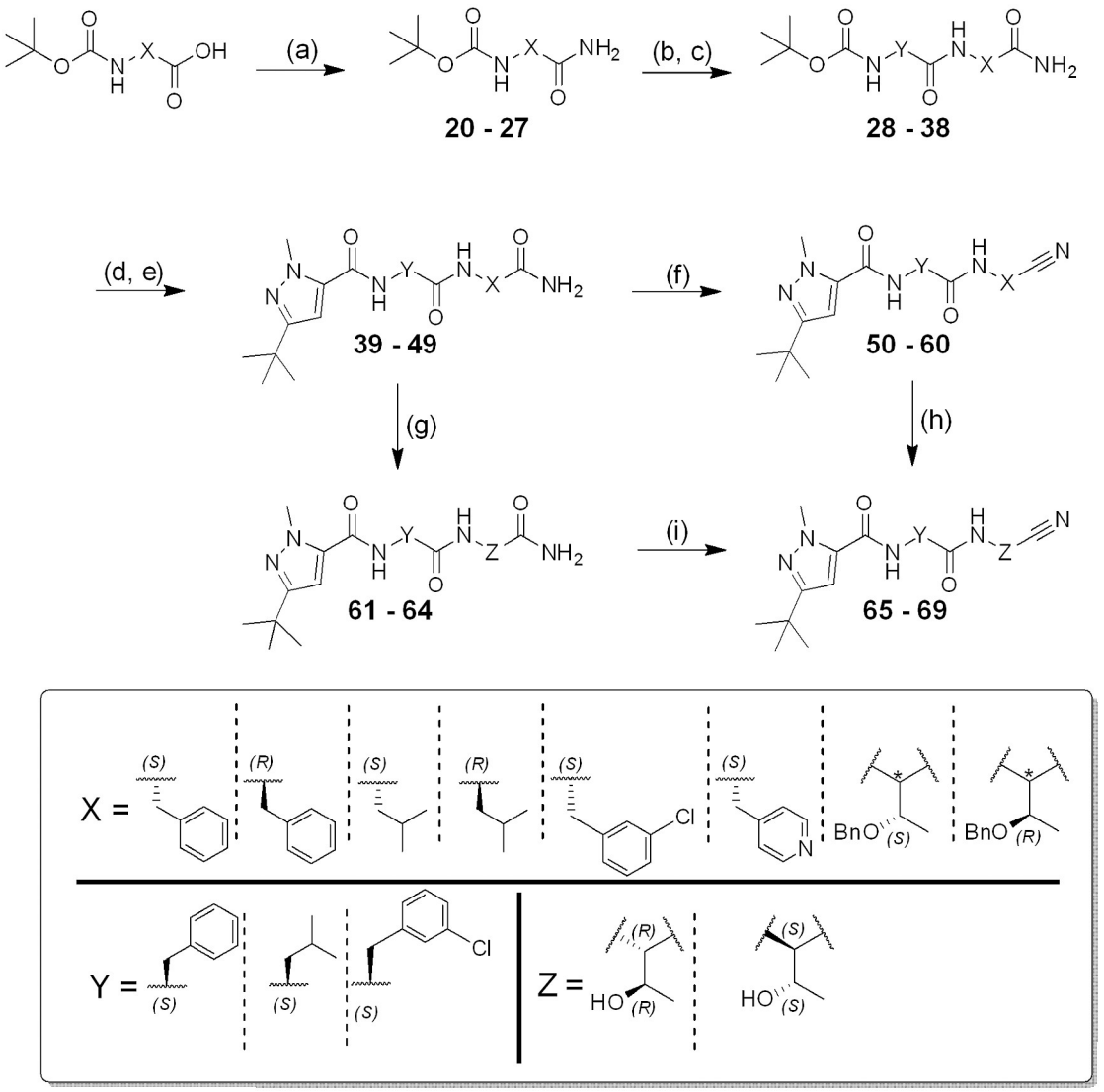

Fig 2. General synthesis of compounds 50–60, 65–69. Reagents and conditions: a) Isobutyl chloroformate, NH_4Cl 2 M, DIPEA, DMF, 0 ˚C to rt, 20 h; b) TFA, CH_2Cl_2, 0 ˚C to rt, 2 h; c) HATU, DIPEA, Boc-AA-OH, DMF, rt, 18 h; d) TFA, CH_2Cl_2, 0 ˚C to rt, 2 h; e)TBTU, DIPEA, 3-(*tert*-butyl)-1-methyl-1*H*-pyrazole-5-carboxylic acid, DMF/CH_2Cl_2, rt, 18 h; f) Cyanuric chloride, DMF, 0 ˚C to rt, 0.5 h; g) H_2 (1 atm), Pd/C, rt, 18 h; h) DDQ, CH_2Cl_2, rt, 3–5 days; i) TFAA, DIPEA, THF, 0 ˚C to rt, 2 h.

https://doi.org/10.1371/journal.pntd.0007755.g002

(100 mL) was added, and it was washed with a saturated $NaHCO_3$ solution (3 × 50 mL) and brine (1 × 50 mL). The organic phase was dried over Na_2SO_4 and evaporated under reduced pressure to give a crude residue that was purified by flash column chromatography.

Method B: The free primary amine (1.0 mmol, 1.0 equiv.) was added to a solution of the carboxylic acid (1.3 mmol, 1.3 equiv.), HATU (490 mg, 1.3 mmol, 1.3 equiv.) and DIPEA (364 mg, 0.45 mL, 2.60 mmol, 2.6 equiv.) in dry DMF (5 mL) under argon atmosphere. The resulting solution was stirred at room temperature for 20 h. The reaction mixture was diluted with ethyl acetate (10 mL) and washed with a saturated $NaHCO_3$ solution (3 × 20 mL) and brine (3 × 20 mL). The organic phase was dried over Na_2SO_4 and evaporated to give a crude residue that was purified by flash column chromatography.

Method C: The free primary amine (1.0 mmol, 1.0 equiv.) was added to a solution of the carboxylic acid (1.3 mmol, 1.3 equiv.), TBTU (410 mg, 1.30 mmol, 1.3 equiv.) and DIPEA (364 mg, 0.45 mL, 2.60 mmol) in dry DMF/CH_2Cl_2 (1:1, 10 mL) under argon atmosphere. The

resulting solution was stirred at room temperature for 20 h. The reaction mixture was diluted with ethyl acetate (10 mL) and washed with a saturated $NaHCO_3$ solution (3 × 20 mL) and brine (3 × 20 mL). The organic phase was dried over Na_2SO_4 and evaporated to give a crude residue that was purified by flash column chromatography.

General procedure for removal of the Boc protecting group. **Method A**: The Boc-protected amino compound (0.25 mmol, 1.0 equiv.) was treated with formic acid (2.44 g, 2.0 mL, 47.9 mmol, 47.9 equiv.) at room temperature. The resulting solution was stirred for 18 h. The reaction mixture was evaporated under reduced pressure to get a yellowish oil. It was treated with an aqueous solution of 1.0 M NaOH until pH 9 was reached. The product was extracted with ethyl acetate (4 × 20 mL) and then washed with brine (1 × 20 mL). The organic phase was evaporated to obtain a colorless oil. The formation of the product was confirmed by TLC (ethyl acetate). The product was used for the next step without further purification.

Method B: To a solution of Boc-protected amino compound (1.0 mmol, 1.0 equiv.) in dry CH_2Cl_2 (3 mL) was added TFA (912 mg, 0.91 mL, 8.00 mmol, 8.0 equiv.) at 0 ˚C. The mixture was stirred and allowed to reach room temperature within exposed mainly h. The progress of the reaction was monitored by TLC (ethyl acetate). The reaction mixture was evaporated under reduced pressure to eliminate the excess of TFA to get a yellowish solid. The product was used for the next step without further purification.

General procedure for dehydration of primary amides to nitriles. **Method A**: The primary amide (1.0 mmol, 1.0 equiv.) was dissolved in dry DMF (5 mL) at 0 ˚C. Then, cyanuric chloride (73 mg, 0.4 mmol, 1.1 equiv.) was slowly added to the solution under argon atmosphere. The resulted solution was stirred for 0.5 h. Saturated $NaHCO_3$ solution (30 mL) was added and it was stirred at room temperature for 2 h. The product was extracted with ethyl acetate (2 x 50 mL), and then the reunited organic phases were washed with an aqueous solution of 1.0 M $KHSO_4$ (3 × 20 mL), brine (4 × 30 mL) and dried over Na_2SO_4. The solvent was removed, and the crude product was purified by flash silica gel chromatography.

Method B: The primary amide (1.0 mmol, 1.0 equiv.) was dissolved in dry THF (5 mL) and DIPEA (364 mg, 0.45 mL, 2.6 mmol, 2.6 equiv.) was added. Trifluoroacetic anhydride (273 mg, 0.18 mL, 1.30 mmol, 1.3 equiv.) was added over 5 min, at 0 ˚C. The mixture was stirred and allowed to reach room temperature within 2 h. Then the reaction was quenched with H_2O (20 mL), THF removed in vacuo, and the product was extracted into ethyl acetate (2 × 50 mL). The organic phase was washed with a solution 1.0 M of $KHSO_4$ (3 × 20 mL) and with a saturated $NaHCO_3$ solution (3 × 20 mL) and brine (3 × 20 mL) and dried over Na_2SO_4. The solvent was removed, and the crude product was purified by flash silica gel chromatography.

Method C: The primary amide (1.0 mmol, 1.0 equiv.) was dissolved in dry pyridine (5 mL) at room temperature. Then, *p*-toluenesulfonyl chloride (572 mg, 3.0 mmol, 3.0 equiv.) was added to the solution under argon atmosphere. The resulting solution was stirred for 3 days. Upon the addition of a saturated $NaHCO_3$ solution (30 mL), the reaction mixture was stirred at room temperature for 2 h. The solution was dried under reduced pressure. The product was extracted with ethyl acetate (2 × 50 mL), and then the reunited organic phases were washed with a 1.0 M solution of $KHSO_4$ (2 × 20 mL), brine (4 × 30 mL) and dried over Na_2SO_4. The solvent was removed, and the crude product was purified by flash silica gel chromatography.

General procedure for removal of the benzyl protecting group. **Method A**: The corresponding protected threonine (1.0 mmol, 1.0 equiv.) was dissolved in ethanol absolute (20 mL) in an argon atmosphere. Upon addition of 10% Pd/C, H_2 was bubbled in the solution for 0.5 h. The resulting solution was stirred under H_2 atmosphere for 12 h. The progress of the reaction was monitored by TLC (ethyl acetate). The solution was filtered on celite two times and dried under reduced pressure to afford the desired product as a colorless wax. The product was used for the next step without further purification.

Method B: The corresponding protected threonine (1.0 mmol, 1.0 equiv.) was dissolved in dry CH_2Cl_2 (20 mL) under argon atmosphere. Then, DDQ (908 mg, 4.0 mmol, 4.0 equiv.) was added, and the resulting solution was stirred for 4 days at room temperature. The progress of the reaction was monitored by TLC (ethyl acetate). The reaction was quenched with an aqueous 1.0 M solution of $NaHSO_3$ (20 mL). Then, CH_2Cl_2 was removed under reduced pressure. The product was extracted with ethyl acetate (2 × 50 mL), and the reunited organic phases were washed with an aqueous solution of 1.0 M $KHSO_4$ (2 × 20 mL), brine (4 × 30 mL) and dried over Na_2SO_4. The solvent was removed, and the crude product was purified by flash silica gel chromatography.

Synthesis and characterization of compound 1–5. Compounds **1–5** have been synthesized from the corresponding amino acid and 1-amino-1-cyclopropanecarbonitrile following the general procedure for amide synthesis (method B) [15].

(S)-tert-Butyl (1-((1-cyanocyclopropyl)amino)-1-oxo-3-phenylpropan-2-yl)carbamate (1). Yield 92%. White solid. R_f = 0.9 (ethyl acetate: *n*-hexane; 7:3). Mp. 146–147 ˚C. ^{1}H NMR (500 MHz, $CDCl_3$) δ 7.27–7.04 (m, 5H), 4.58 (m, 1H), 3.19 (dd, *J* = 13.8, 5.0 Hz, 1H), 2.88 (dd, *J* = 9.5, 5.0 Hz, 1H), 1.31 (s, 9H), 1.25 (m, 2H), 1.04 (m, 2H). ^{13}C NMR. (125 MHz, $CDCl_3$) δ 173.06, 155.30, 137.73, 129.35, 128.19, 126.45, 120.80, 78.30, 55.54, 37.36, 28.26, 19.77, 15.80, 15.75. ESI-MS (+) Calc. for $[C_{18}H_{23}N_3O_3]$ 329.39, found: 352.3 $[M+Na]^+$.

(S)-tert-Butyl (3-(3-chlorophenyl)-1-((1-cyanocyclopropyl)amino)-1-oxopropan-2-yl) carbamate (2). Yield 83%. White solid. R_f = 0.7 (ethyl acetate: *n*-hexane; 6:4). Mp. 146–147 ˚C. ^{1}H NMR (500 MHz, $CDCl_3$) δ 7.26–7.25 (m, 1H), 7.23–7.21 (m, 1H), 7.08–7.03 (m, 2H), 4.27–4.24 (m, 1H), 3.10 (dd, *J* = 13.8, 5.0 Hz, 1H), 2.83 (dd, *J* = 9.5, 5.0 Hz, 1H), 1.52–1.44 (m, 2H), 1.41 (s, 9H), 1.13–1.05 (m, 2H). ^{13}C NMR (125 MHz, $CDCl_3$) 172.02, 155.61, 138.23, 134.32, 129.29, 127.49, 127.25, 119.48, 119.48, 80.55, 55.28, 37.87, 28.18, 20.14, 16.68, 16.56. ESI-MS (+) Calc. for $[C_{18}H_{22}ClN_3O_3]$ 363.83, found: 364.3 $[M+H]^+$.

(S)-tert-Butyl (1-((1-cyanocyclopropyl)amino)-1-oxo-3-(pyridin-4-yl)propan-2-yl)carbamate (3). Yield 75%. White solid. R_f = 0.5 (ethyl acetate: *n*-hexane; 4:6). Mp. 134–135 ˚C. ^{1}H NMR (200 MHz, CD_3OD) δ 8.45 (d, *J* = 4.9 Hz, 2H), 7.34 (d, *J* = 5.8 Hz, 2H), 4.36–4.23 (m, 1H), 2.96 (dd, *J* = 14.0, 5.0 Hz, 2H), 1.53–1.46 (m, 1H), 1.38 (s, 9H), 1.20–1.14 (m, 2H). ^{13}C NMR (50 MHz, $CDCl_3$) δ 174.74, 149.95, 149.15, 126.52, 121.09, 80.79, 56.03, 38.88, 38.31, 28.55, 21.21, 17.05. ESI-MS (+) Calc. for $[C_{17}H_{22}N_4O_3]$ 330.38, found: 331.2 $[M+H]^+$.

(S)-tert-Butyl (1-((1-cyanocyclopropyl)amino)-4-methyl-1-oxopentan-2-yl)carbamate (4). Yield 61%. White solid. R_f = 0.7 (ethyl acetate: *n*-hexane; 4:6). Mp. 162–164 ˚C. ^{1}H NMR (500 MHz, DMSO-d_6) δ 8.76 (s, 1H), 6.86 (d, *J* = 7.9 Hz, 1H), 3.86 (dt, *J* = 8.7, 5.5 Hz, 1H), 1.55–1.54 (m, *J* = 6.6 Hz, 1H), 1.44 (dd, *J* = 7.9, 5.5 Hz, 2H), 1.37–1.42 (m, 2H), 1.36 (s, 9H), 1.07 (dd, *J* = 7.7, 5.3 Hz, 2H), 0.84 (2d, *J* = 6.6 Hz, 6H). ^{13}C NMR (125 MHz, DMSO-d_6) δ 174.17, 155.50, 120.92, 78.22, 52.58, 40.49, 28.31, 24.38, 23.01, 21.66, 19.91, 15.87, 15.75. ESI-MS (+) Calc. for $[C_{15}H_{25}N_3O_3]$ 295.37, found: 318.3 $[M+Na]^+$.

tert-Butyl ((2S,3R)-3-(benzyloxy)-1-((1-cyanocyclopropyl)amino)-1-oxobutan-2-yl)carbamate (5). Yield 89%. White solid. R_f = 0.7 (ethyl acetate: *n*-hexane; 4:6). Mp. 88–90 ˚C. ^{1}H NMR (200 MHz, $CDCl_3$) δ 7.36–7.32 (m, 5H), 4.78–4.60 (m, 3H), 4.22–4.12 (m, 1H), 1.57–1.44 (m, 2H), 1.30–1.27 (m, 9H), 1.17–1.13 (m, 5H). ESI-MS (+) Calc. for $[C_{20}H_{27}N_3O_4]$ 373.44, found: 396.4 $[M+Na]^+$.

Synthesis of compounds 6–18. Compounds **6–18** have been synthesized in two steps from compounds **1–5**. First, the Boc group was removed (procedure A), and then the free amine was coupled to the carboxylic acid following the general procedure for amide synthesis (method B or method C, as indicated).

Synthesis and characterization of compounds **6**, **9** and **11** have been already published elsewhere [14].

(S)-N-(3-(3-Chlorophenyl)-1-((1-cyanocyclopropyl)amino)-1-oxopropan-2-yl)benzamide (7). Method B. Yield 86%. White solid. R_f = 0.7 (ethyl acetate: *n*-hexane; 6:4). Mp. 213–215 ˚C. ^{1}H NMR (500 MHz, DMSO-d_6) δ 9.04 (s, 1H), 8.67 (d, *J* = 8.1 Hz, 1H), 7.84–7.83 (m, 2H), 7.56–7.54 (m, 1H), 7.53 (t, *J* = 7.7 Hz, 2H), 7.41 (s, 1H), 7.32–7.25 (m, 3H), 4.65–4.60 (m, 1H), 3.09 (dd, *J* = 13.6, 5.0 Hz, 1H), 3.02 (dd, *J* = 15.2, 5.0 Hz, 1H), 1.51–1.49 (m, 2H), 1.12–1.06 (m, 2H). ^{13}C NMR (125 MHz, DMSO-d_6) δ 172.57, 166.48, 140.62, 132.82, 131.52, 130.04, 129.18, 128.31, 128.05, 127.58, 126.50, 120.81, 54.47, 36.60, 19.90, 15.82. HRMS (+) Calc. for $[C_{20}H_{19}ClN_3O_2]^+$ 368.11658, found: 368.11615 $[M+H]^+$. HPLC (protocol B): t_R (min) = 10.29. Purity: 99.6%.

(S)-3-(tert-Butyl)-N-(3-(3-chlorophenyl)-1-((1-cyanocyclopropyl)amino)-1-oxopropan-2-yl)-1-methyl-1H-pyrazole-5-carboxamide (8). Method C. Method B. Yield 72%. Yellowish solid. R_f = 0.7 (ethyl acetate: *n*-hexane; 5:5). Mp. 152–154 ˚C. ^{1}H NMR (400 MHz, DMSO-d_6) δ 9.03 (s, 1H), 8.59 (d, *J* = 8.4 Hz, 1H), 7.39 (s, 1H), 7.31–7.24 (m, 3H), 6.79 (s, 1H), 4.57–4.53 (m, 1H), 3.88 (s, 3H), 3.08 (dd, *J* = 13.6, 5.1 Hz, 1H), 2.94 (dd, *J* = 13.6, 10.2 Hz, 1H), 1.50–1.47 (m, 2H), 1.28 (s, 9H), 1.10–1.05 (m, 2H). ^{13}C NMR (100 MHz, DMSO-d_6) δ 172.10, 159.46, 158.70, 140.26, 134.95, 132.64, 129.94, 129.15, 127.85, 126.39, 120.63, 103.82, 55.21, 36.38, 31.58, 30.36, 19.75, 15.67, 15.61. HRMS (+) Calc. for $[C_{22}H_{27}ClN_5O_2]^+$ 428.18533, found: 428.1864 $[M+H]^+$. HPLC (protocol B): t_R (min) = 11.17. Purity: 98.3%.

(S)-3-(tert-Butyl)-N-(1-((1-cyanocyclopropyl)amino)-1-oxo-3-(pyridin-4-yl)propan-2-yl)-1-methyl-1H-pyrazole-5-carboxamide (10). Method C. Yield 56%. Yellowish oil. R_f = 0.4 (ethyl acetate: *n*-hexane; 5:5). ^{1}H NMR (200 MHz, CD_3OD) δ 8.48–8.46 (m, 2H), 7.43 (d, *J* = 4.9 Hz, 2H), 6.69 (s, 1H), 4.86–4.78 (m, 1H), 3.95 (s, 3H), 3.04–3.02 (m, 1H), 2.89–2.84 (m, 1H), 1.56–1.50 (m, 2H), 1.31 (d, *J* = 4.3 Hz, 9H), 1.22–1.18 (m, 2H). ^{13}C NMR (50 MHz, CD_3OD) δ 172.80, 160.35, 160.05, 148.62, 147.59, 134.80, 125.00, 119.66, 103.60, 53.18, 37.37, 36.45, 31.42, 29.44, 19.92, 15.60, 15.28. FT-IR (KBr, cm^{-1}) 3297.16, 2966.17, 2242.31, 1670.63, 1601.36, 1531.90, 1425.65, 1352.10, 1278.55, 1241.77, 1049.72, 988.42, 808.63, 755.51, 722.82, 511.19, 506.24, 489.90. HRMS (+) Calc. for $[C_{21}H_{27}N_6O_2]^+$ 395.21955, found: 395.21973 $[M+H]^+$. HPLC (protocol B): t_R (min) = 3.68. Purity: 94.7%.

N-((2S,3R)-3-(Benzyloxy)-1-((1-cyanocyclopropyl)amino)-1-oxobutan-2-yl)-3-(tert-butyl)-1-methyl-1H-pyrazole-5-carboxamide (12). Method C. Yield 53%. Yellowish solid. R_f = 0.4 (ethyl acetate: *n*-hexane; 6:4). Mp. 100–101 ˚C. ^{1}H NMR (200 MHz, $CDCl_3$) δ 7.36–7.32 (m, 5H), 6.45 (s, 1H), 4.76–4.62 (m, 3H), 4.22–4.12 (m, 1H), 4.09 (s, 3H), 1.57–1.44 (m, 2H), 1.30–1.27 (m, 9H), 1.20–1.13 (m, 5H). ^{13}C NMR (50 MHz, $CDCl_3$) δ 170.36, 160.18, 159.74, 137.15, 134.06, 128.48, 127.98, 127.68, 119.25, 103.18, 74.03, 71.48, 54.81, 38.38, 31.66, 30.16, 28.68, 20.24, 16.91, 15.85. FT-IR (KBr, cm^{-1}) 3288.99, 2953.92, 2917.14, 2214.31, 1646.31, 1589.10, 1495.12, 1049.31, 1294.89, 1200.91, 1033.37, 922.51, 755.51, 681.95. HRMS (+) Calc. for $[C_{24}H_{32}N_5O_3]^+$ 437.25051, found: 438.25102 $[M+H]^+$. HPLC (protocol B): t_R (min) = 8.77. Purity: 97.0%.

(S)-7-Chloro-N-(1-((1-cyanocyclopropyl)amino)-1-oxo-3-phenylpropan-2-yl)quinoline-4-carboxamide (13). Method B. Yield 74%. White solid. R_f = 0.7 (ethyl acetate: *n*-hexane; 8:2). Mp. 260–262 ˚C. ^{1}H NMR (400 MHz, DMSO-d_6) δ 9.15 (d, *J* = 10.2 Hz, 1H), 9.13 (s, 1H), 8,97 (d, *J* = 10.2 Hz, 1H), 8.10 (d, *J* = 2.1 Hz, 1H), 7.72 (d, *J* = 15 Hz, 1H), 7.56 (dd, *J* = 15.1, 10.2 Hz, 1H), 7.44 (d, *J* = 10.2 Hz, 1H), 7.28–7.24 (m, 5H), 4.75–4.73 (m, 1H), 3.11 (dd, *J* = 13.8, 5.0 Hz, 1H), 2.87 (dd, *J* = 9.5, 5.0 Hz, 1H), 1.51–1.49 (m, 2H), 1.09–1.07 (m, 1H). ^{13}C NMR (100 MHz, DMSO-d_6) δ 172.34, 166.33, 151.74, 148.36, 141.88, 137.63, 134.53, 129.45, 128.42, 128.00, 127.86, 126.74, 122.89, 120.91, 119.69, 54.56, 37.26, 20.02, 15.89. FT-IR (KBr, cm^{-1}) 3254.05, 2926.14, 2247.17, 1672.36, 1668.36, 1523.83, 846.79, 831.36. HRMS (+) Calc. for $[C_{23}H_{20}ClN_4O_2]^+$ 418.12748, found: 419.12813 $[M+H]^+$. HPLC (protocol C, 50:50 ACN: water): t_R (min) = 17.32. Purity: 99.9%.

(S)-7-Chloro-N-(1-((1-cyanocyclopropyl)amino)-3-(1H-indol-3-yl)-1-oxopropan-2-yl) quinoline-4-carboxamide (14). Method B. Yield 49%. Yellowish solid. R_f = 0.3 (ethyl acetate). Mp. 196–197 ˚C. ^{1}H NMR (400 MHz, DMSO-d_6) δ 10.88 (s, 1H), 9.15 (s, 1H), 9.08 (d, *J* = 10.2 Hz, 1H), 8.97 (d, *J* = 4.2 Hz, 1H), 8.10 (d, *J* = 2.2 Hz, 1H), 7.68 (t, *J* = 7.5 Hz, 1H), 7.54–7.52 (m, 1H), 7.46 (d, *J* = 4.5 Hz, 1H), 7.38 (d, *J* = 10.2 Hz 1H), 7.16 (d, *J* = 2.4 Hz, 1H), 7.09 (t, *J* = 5.5 Hz, 1H), 7.00 (t, *J* = 5.8 Hz, 1H), 4.81–4.79 (m, 1H), 3.20 (dd, *J* = 13.8, 5.0 Hz, 1H), 3.05 (dd, *J* = 9.5, 5.0 Hz, 1H), 1.51–1.48 (m, 2H), 1.11–1.08 (m, 2H). ^{13}C NMR (100 MHz, DMSO-d_6) δ 173.02, 166.59, 151.94, 148.61, 142.38, 136.57, 134.72, 128.23, 128.05, 128.03, 127.52, 124.56, 123.19, 121.46, 121.26, 119.97, 119.03, 118.76, 111.81, 110.02, 54.26, 27.79, 20.33, 16.20. FT-IR (KBr, cm^{-1}) 3254.05, 2926.14, 2247.17, 1672.36, 1665.34, 1522.83, 831.30, 732.98. HRMS (+) Calc. for $[C_{25}H_{21}ClN_5O_2]^+$ 458.13838, found: 458.13703 $[M+H]^+$. HPLC (protocol C, 50:50 ACN: water): t_R (min) = 18.64. Purity: 99.6%.

(S)-7-Chloro-N-(1-((1-cyanocyclopropyl)amino)-4-methyl-1-oxopentan-2-yl)quinoline-4-carboxamide (15). Method B. Yield 68%. White solid. R_f = 0.7 (ethyl acetate). Mp. 169–170 ˚C. ^{1}H NMR (400 MHz, DMSO-d_6) δ 9.10 (s, 1H), 9.05 (s, 1H), 9.02 (d, *J* = 5.5 Hz, 1H) 8.20 (d, *J* = 11.5 Hz, 1H), 8.15 (d, *J* = 2.5 Hz, 1H), 7.72 (dd, *J* = 11.5, 2.5 Hz, 1H), 7.60 (d, *J* = 5.5 Hz, 1H), 4.48–4.46 (m, 1H), 1.70–1.63 (m, 3H), 1.52–1.48 (m, 2H), 1.19–1.14 (m, 2H), 0.92 (2d, *J* = 10.5 Hz, 6H). ^{13}C NMR (100 MHz, DMSO-d_6) δ 173.63, 166.83, 152.05, 148.70, 142.06, 134.83, 131.26, 128.38, 123.35, 121.21, 120.20, 51.97, 24.87, 23.38, 21.79, 20.34, 16.22, 16.06. FT-IR (KBr, cm^{-1}) 3402.4, 3257.7, 3030.1, 2960.7, 2247.0, 1674.2, 1633.7, 1529.5, 1296.1, 831.31. HRMS (+) Calc. for $[C_{20}H_{22}ClN_4O_2]^+$ 384.14313, found: 385.14503 $[M+H]^+$. HPLC (protocol C, 65:35 ACN: water): t_R (min) = 11.81. Purity: 96.2%.

(S)-3-((1-((1-Cyanocyclopropyl)amino)-1-oxo-3-phenylpropan-2-yl)carbamoyl)phenyl benzoate (16). Method B. Yield 89%. White solid. R_f = 0.7 (ethyl acetate: *n*-hexane; 6:4). Mp. 185–187 ˚C. ^{1}H NMR (400 MHz, DMSO-d_6) δ 9.05 (s, 1H), 8.79 (d, *J* = 8.0 Hz, 1H), 8.18–8.16 (m, 2H), 7.81–7.78 (m, 3H), 7.64 (t, *J* = 8.5 Hz, 2H), 7.57 (t, *J* = 8.5 Hz, 2H), 7.50–7.48 (m, 1H), 7.31–7.23 (m, 4H), 7.18 (tt, *J* = 7.0, 1.5 Hz, 1H), 4.64–4.59 (m, 1H), 3.06 (dd, *J* = 13.6, 5.0 Hz, 1H), 3.00 (dd, *J* = 13.5, 8.5 Hz, 1H), 1.49–1.45 (m, 2H), 1.06–1.01 (m, 2H). ^{13}C NMR (100 MHz, DMSO-d_6) δ 173.04, 165.60, 165.02, 150.88, 138.21, 135.72, 134.66, 130.27, 129.98, 129.57, 129.51, 129.16, 128.57, 126.83, 125.69, 125.53, 121.47, 121.15, 55.10, 37.36, 20.18, 16.15, 16.10, 14.55. FT-IR (KBr, cm^{-1}) 3254.05, 2926.14, 2247.17, 1672.36, 1668.36, 1523.83, 846.79, 831.36. HRMS (+) Calc. for $[C_{27}H_{24}N_3O_4]^+$ 453.17668, found: 454.17800 $[M+H]^+$. HPLC (protocol C, 65:35 ACN: water): t_R (min) = 19.62. Purity: 99.9%.

(S)-6-Amino-N-(1-((1-cyanocyclopropyl)amino)-4-methyl-1-oxopentan-2-yl)nicotinamide (17). Method C. Yield 48%. Yellowish solid. R_f = 0.3 (ethyl acetate: methanol; 8:2). Mp. 100–101 ˚C. ^{1}H NMR (200 MHz, CD_3OD) δ 8.43 (s, 1H), 7.88 (d, *J* = 8.8, 2.1 Hz, 1H), 6.54 (d, *J* = 8.9 Hz,1H), 4.53–4.46 (m, 1H), 1.82–1.51 (m, 3H), 1.47–1.43 (m, 2H), 1.24–1.17 (m, 2H), 0.96–0.93 (m, 6H). ^{13}C NMR (50 MHz, CD_3OD) δ 176.59, 168.58, 162.86, 149.21, 138.44, 121.42, 119.42, 109.12, 41.60, 26.13 23.54, 21.98, 21.41, 17.15, 16.78. FT-IR (KBr, cm^{-1}) 3288.99, 2953.92, 2917.14, 2214.31,1647.63, 1496.06, 1409.33, 1294.89, 1202.33, 1075.33, 1030.81, 922.54, 763.49, 667.21. ESI-MS (+) Calc. for $[C_{16}H_{22}N_5O_2]^+$ 316.17735, found: 316.17713 $[M+H]^+$. HPLC (protocol B): t_R (min) = 8.77. Purity: 97.0%.

(S)-N-(1-((1-Cyanocyclopropyl)amino)-4-methyl-1-oxopentan-2-yl)-1H-pyrrolo[2,3-b] pyridine-5-carboxamide (18). Method C. Yield 45%. White solid. R_f = 0.3 (ethyl acetate: methanol; 8:2). Mp. 79–80 ˚C. ^{1}H NMR (200 MHz, CD_3OD) δ 8.71 (d, *J* = 1.8 Hz, 1H), 8.47 (d, *J* = 2.0 Hz, 1H), 7.46 (d, *J* = 3.5 Hz, 1H), 6.57 (d, *J* = 3.5 Hz, 1H), 4.59–4.57 (m, 1H), 1.91–1.56 (m, 3H), 1.54–1.49 (m, 2H), 1.29–1.25 (m, 2H), 1.01–0. 89 (m, 6H). ^{13}C NMR (50 MHz, CD_3OD) δ 176.50, 169.61, 163.45, 150.38, 143.32, 129.52, 128.65, 123.21, 120.94, 102.66, 53.50, 38.92, 26.18, 23.41, 22.02, 21.25, 17.17, 16.49. FT-IR (KBr, cm^{-1}) 3286.44, 2933.89, 2924.14,

2216.51, 1647.63, 1588.10, 1496.06, 1409.33, 1294.89, 1202.33, 1075.33, 1030.31, 922.54, 763.54, 667.21. ESI-MS (+) Calc. for $[C_{18}H_{22}N_5O_2]^+$ 340.17753, found: 340.17689 $[M+H]^+$. HPLC (protocol B): t_R (min) = 5.38. Purity: 99.0%.

Synthesis and characterization of compound 19. Compound **19** has been synthesized from compound **12** by removal of the benzyl protecting group under mild conditions (protocol B).

3-(tert-Butyl)-N-((2S,3R)-1-((1-cyanocyclopropyl)amino)-3-hydroxy-1-oxobutan-2-yl)-1-methyl-1H-pyrazole-5-carboxamide (19). Yield 40%. Yellowish solid. R_f = 0.3 (ethyl acetate). Mp. 201–202 ˚C. ^{1}H NMR (200 MHz, CD_3OD) δ 6.81 (s, 1H), 4.40 (d, *J* = 4.4 Hz, 1H), 4.23–4.18 (m, 1H), 4.04 (s, 3H), 1.52–1.47(m, 2H), 1.32 (s, 9H), 1.29–1.18 (m, 5H). ^{13}C NMR (50 MHz, CD_3OD) δ 174.94, 163.34, 162.74, 137.60, 122.22, 106.16, 69.42, 61.17, 39.91, 34.00, 31.94, 22.41, 21.45, 18.11, 17.83. FT-IR (KBr, cm^{-1}) 3288.89, 2953.92, 2917.14, 2214.31, 1646.31, 1589.10, 1495.12, 1049.31, 1294.89, 1200.91, 1033.97, 922.51, 755.51, 681.95. ESI-MS (-) Calc. for $[C_{17}H_{25}N_5O_3]^+$ 348.20356, found: 348.20314 $[M+H]^+$. HPLC (protocol B): t_R (min) = 7.74. Purity: 98.0%.

Synthesis of compounds 20–27. Compounds **20**–**27** have been synthesized from the equivalent amino Boc-protected amino acid following the general procedure for amide synthesis (method A).

(S)-tert-Butyl (1-amino-1-oxo-3-phenylpropan-2-yl)carbamate (20). Yield 77%. White solid. R_f = 0.6 (ethyl acetate). Mp. 146–149 ˚C. ^{1}H NMR (200 MHz, CD_3OD) δ 7.26–7.16 (m, 5H), 4.44–4.41 (m, 1H), 3.14 (dd, *J* = 13.7, 6.0 Hz, 1H), 2.88 (dd, *J* = 13.7, 8.1 Hz, 1H), 1.23 (s, 9H). ^{13}C NMR (50 MHz, CD_3OD) δ 173.98, 155.60, 130.73, 124.93, 122.46, 118.22, 80.20, 54.02, 37.73, 27.94. ESI-MS (+) Calc. for $[C_{14}H_{20}N_2O_3]$ 264.31, found: 287.3 $[M+Na]^+$.

(R)-tert-butyl (1-amino-1-oxo-3-phenylpropan-2-yl)carbamate (21). Yield 79%. White solid. R_f = 0.6 (ethyl acetate). Mp. 141–142 ˚C. ^{1}H NMR (200 MHz, CD_3OD) δ 7.24–7.17 (m, 5H), 4.42–4.37 (m, 1H), 3.14 (dd, *J* = 13.7, 6.0 Hz, 1H), 2.92 (dd, *J* = 13.7, 8.1 Hz, 1H), 1.43 (s, 9H). ^{13}C NMR (50 MHz, CD_3OD) δ 173.12, 154.48, 133.36, 122.46, 121.75, 119.38, 83.51, 55.61, 38.38, 28.66. ESI-MS (+) Calc. for $[C_{14}H_{20}N_2O_3]$ 264.31, found: 287.3 $[M+Na]^+$.

(S)-tert-Butyl (1-amino-4-methyl-1-oxopentan-2-yl)carbamate (22). Yield 74%. White solid. R_f = 0.4 (ethyl acetate). Mp. 138–141 ˚C. ^{1}H NMR (200 MHz, $CDCl_3$) δ 6.58 (s br, 1H), 6.13 (s br, 1H), 5.25–4.97 (m, 2H), 4.15 (s br, 1H), 1.73–1.43 (m, 3H), 1.41 (s, 9H), 0.92 (d, *J* = 3.2 Hz, 6H). ^{13}C NMR (50 MHz, $CDCl_3$) δ 172.34, 155.95, 71.56, 28.57, 28.18, 25.08, 23.21, 19.25. ESI-MS (+) Calc. for $[C_{11}H_{22}N_2O_3]$ 230.30, found: 253.3 $[M+Na]^+$.

(R)-tert-Butyl (1-amino-4-methyl-1-oxopentan-2-yl)carbamate (23). Yield 71%. White solid. R_f = 0.4 (ethyl acetate). Mp. 138–141 ˚C. ^{1}H NMR (200 MHz, $CDCl_3$) δ 6.64 (s br, 1H), 6.21 (s br, 1H), 5.21–4.98 (m, 2H), 4.16 (s br, 1H), 1.71–1.45 (m, 3H), 1.42 (s, 9H), 0.93 (d, *J* = 3.2 Hz, 6H). ^{13}C NMR (50 MHz, $CDCl_3$) δ 172.11, 155.37, 71.64, 28.61, 28.29, 25.15, 23.34, 19.30. ESI-MS (+) Calc. for $[C_{11}H_{22}N_2O_3]$ 230.30, found: 253.3 $[M+Na]^+$.

(S)-tert-Butyl (1-amino-3-(3-chlorophenyl)-1-oxopropan-2-yl)carbamate (24). Yield 74%. White solid. R_f = 0.4 (ethyl acetate). Mp. 111–112 ˚C. ^{1}H NMR (200 MHz, $CDCl_3$) δ 7.26–7.13 (m, 4H), 6.16 (s, 1H), 5.75 (s, 1H), 5.21 (d, *J* = 7.8 Hz, 1H), 4.42–4.36 (m, 1H), 3.19–2.94 (m, 2H), 1.44 (s, 9H). ^{13}C NMR (50 MHz, $CDCl_3$) δ 173.53, 155.16, 138.90, 134.09, 130.04, 129.44, 127.55, 127.11, 80.31, 37.88, 28.16. ESI-MS (+) Calc. for $[C_{14}H_{19}ClN_2O_3]$ 298.77, found: 321.8 $[M+Na]^+$.

(S)-tert-Butyl (1-amino-1-oxo-3-(pyridin-4-yl)propan-2-yl)carbamate (25). Yield 92%. White solid. R_f = 0.2 (ethyl acetate). Mp. 131–133 ˚C. ^{1}H NMR (200 MHz, $CDCl_3$) δ 8.42 (d, *J* = 5.7 Hz, 2H), 7.22 (d, *J* = 5.9 Hz, 2H), 4.35–4.31 (m, 1H), 3.18 (dd, *J* = 13.7, 6.0 Hz, 1H), 2.81 (dd, *J* = 13.7, 8.1 Hz, 1H), 1.49–1.33 (s br, 9H). ^{13}C NMR (50 MHz, $CDCl_3$) δ 173.69, 155.86,

148.48, 147.61, 118.42, 80.22, 54.51, 37.77, 27.89. ESI-MS (+) Calc. for $[C_{13}H_{19}N_3O_3]$ 265.31, found: 266.2 $[M+H]^+$.

tert-Butyl ((2S,3R)-1-amino-3-(benzyloxy)-1-oxobutan-2-yl)carbamate (26). Yield 65%. White solid. R_f = 0.5 (ethyl acetate). Mp. 145–147 ˚C. ^{1}H NMR (500 MHz, $CDCl_3$) δ 7.37–7.28 (m, 5H), 6.50 (s, 1H), 5.70–5.51 (m, 2H), 4.62 (q, *J* = 4.6 Hz, 2H), 4.34–4.31 (m, 1H), 4.18–4.11 (m, 1H), 1.45 (s, 9H), 1.19 (d, *J* = 6.3 Hz, 3H). ^{13}C NMR (125 MHz, $CDCl_3$) δ 172.09, 155.66, 137.78, 128.41, 127.82, 127.73, 80.03, 74.53, 71.61, 57.13, 28.23, 27.84, 18.92. ESI-MS (+) Calc. for $[C_{16}H_{24}N_2O_4]$ 308.37, found: 331.4 $[M+Na]^+$.

tert-Butyl ((2R,3S)-1-amino-3-(benzyloxy)-1-oxobutan-2-yl)carbamate (27). Yield 68%. White solid. R_f = 0.5 (ethyl acetate). Mp. 143–145 ˚C. ^{1}H NMR (500 MHz, $CDCl_3$) δ 7.37–7.28 (m, 5H), 6.50 (s, 1H), 5.70–5.51 (m, 2H), 4.62 (q, *J* = 4.6 Hz, 2H), 4.33 (s br, 1H), 4.27–4.19 (m, 1H), 1.45 (s, 9H), 1.19 (d, *J* = 6.3 Hz, 3H) .^{13}C NMR (125 MHz, $CDCl_3$) δ 172.74, 156.31, 138.44, 129.06, 128.47, 128.38, 80.68, 77.16, 75.18, 72.26, 57.78, 28.89, 28.49, 19.57. ESI-MS (+) Calc. for $[C_{16}H_{24}N_2O_4]$ 308.37, found: 331.4 $[M+Na]^+$.

Synthesis of compounds 28–38. Compounds **28**–**38** have been synthesized in two steps from their precursors **20**–**27**. After removal of the Boc-protecting group (method B), the resulting free amine was coupled to the carboxylic acid following the general procedure for amide synthesis (method B).

tert-Butyl ((S)-1-(((S)-1-amino-1-oxo-3-phenylpropan-2-yl)amino)-1-oxo-3-phenylpropan-2-yl)carbamate (28). Yield 92%. White solid. R_f = 0.8 (ethyl acetate). Mp. 186–188 ˚C. ^{1}H NMR (200 MHz, CD_3OD) δ 7.37–7.22 (m, 6H), 7.16–7.09 (m, 4H), 4.76–4.63 (m, 1H), 4.34–4.20 (m, 1H), 3.15–2.95 (m, 2H), 2.91–2.62 (m, 2H), 1.39 (s, 9H). ^{13}C NMR (50 MHz, CD_3OD) δ 174.36, 172.35, 156.09, 136.44, 129.04, 128.35, 128.27, 126.78, 126.64, 79.89, 56.00, 53.78, 37.73, 37.24, 27.84. ESI-MS (+) Calc. for $[C_{23}H_{29}N_3O_4]$ 411.49, found: 434.3 $[M+Na]^+$.

tert-Butyl ((S)-1-(((R)-1-amino-1-oxo-3-phenylpropan-2-yl)amino)-1-oxo-3-phenylpropan-2-yl)carbamate (29). Yield 92%. White solid. R_f = 0.8 (ethyl acetate). Mp. 185–187 ˚C. ^{1}H NMR (200 MHz, CD_3OD) δ 7.75–7.60 (m, 6H), 7.56–7.49 (m, 4H), 5.14–5.01 (m, 1H), 4.72–4.57 (m, 1H), 3.53–3.33 (m, 2H), 3.29–3.00 (m, 2H), 1.77 (s, 9H). ^{13}C NMR (50 MHz, CD_3OD) δ 174.85, 172.83, 156.58, 136.93, 129.53, 128.83, 128.76, 127.26, 127.13, 80.38, 56.49, 54.26, 38.22, 37.73, 28.33. ESI-MS (+) Calc. for $[C_{23}H_{29}N_3O_4]$ 411.49, found: 434.3 $[M+Na]^+$.

tert-Butyl ((S)-1-(((S)-1-amino-4-methyl-1-oxopentan-2-yl)amino)-1-oxo-3-phenylpropan-2-yl)carbamate (30). Yield 83%. White solid. R_f = 0.8 (ethyl acetate). Mp. 164–165 ˚C. ^{1}H NMR (200 MHz, CD_3OD) δ 7.24–7.20 (m, 5H), 4.33–4.28 (m, 1H), 4.11–4.05 (m, 1H), 3.03–2.93 (m, 2H), 1.56–1.38 (m, 2H), 1.36 (s, 9H), 1.26–1.24 (m, 1H), 0.89 (d, *J* = 2.6 Hz, 6H). ^{13}C NMR (50 MHz, CD_3OD) δ 175.39, 154.59, 143.42, 136.55, 128.99, 128.29, 126.65, 84.91, 72.86, 52.36, 51.47, 27.61, 24.41, 22.20, 21.01. ESI-MS (+) Calc. for $[C_{20}H_{31}N_3O_4]$ 377.48, found: 400.5 $[M+Na]^+$.

tert-Butyl ((S)-1-(((R)-1-amino-4-methyl-1-oxopentan-2-yl)amino)-1-oxo-3-phenylpropan-2-yl)carbamate (31). Yield 88%. White solid. R_f = 0.8 (ethyl acetate). Mp. 168–170 ˚C. ^{1}H NMR (200 MHz, CD_3OD) δ 7.24–7.21 (m, 5H), 4.31–4.21 (m, 1H), 4.11–4.09 (m, 1H), 3.04–2.94 (m, 2H), 1.57–1.40 (m, 2H), 1.39 (s, 9H), 1.27–1.24 (m, 1H), 0.90 (d, *J* = 2.6 Hz, 6H). ^{13}C NMR (50 MHz, CD_3OD) δ 175.80, 155.00, 143.83, 136.96, 129.40, 128.70, 127.06, 85.32, 77.16, 73.27, 52.78, 51.89, 28.02, 24.82, 22.61, 21.42. ESI-MS (+) Calc. for $[C_{20}H_{31}N_3O_4]$ 377.48, found: 400.5 $[M+Na]^+$.

tert-Butyl ((S)-1-(((S)-1-amino-3-(3-chlorophenyl)-1-oxopropan-2-yl)amino)-1-oxo-3-phenylpropan-2-yl)carbamate (32). Yield 78%. White solid. R_f = 0.6 (ethyl acetate). Mp. 148–150 ˚C. ^{1}H NMR (200 MHz, $CDCl_3$) δ 7.38–7.26 (m, 7H), 7.10–7.06 (m, 2H), 6.63 (s br, 1H), 6.39 (s br, 1H), 4.81–4.77 (m, 1H), 4.38–4.35 (m, 1H), 3.05–2.97 (m, 4H), 1.41 (s, 9H). ^{13}C NMR (50 MHz, $CDCl_3$) δ 172.83, 161.82, 138.54, 136.14, 134.46, 133.26, 130.05, 129.51,

129.36, 129.02, 127.69, 127.36, 126.78, 80.95, 62.51, 53.21, 52.76, 38.74, 28.23. ESI-MS (+) Calc. for $[C_{23}H_{28}ClN_3O_4]$ 445.94, found: 468.8 $[M+Na]^+$.

tert-Butyl ((S)-1-(((S)-1-amino-1-oxo-3-(pyridin-4-yl)propan-2-yl)amino)-1-oxo-3-phenylpropan-2-yl)carbamate (33). Yield 71%. Yellowish solid. R_f = 0.4 (ethyl acetate). Mp. 155–157 ˚C. ^{1}H NMR (200 MHz, CD_3OD) δ 8.63 (d, *J* = 5.7 Hz, 2H), 7.58–7.30 (m, 7H), 4.94–4.89 (1H, m), 4.55–4.40 (m, 1H), 3.44 (dd, *J* = 13.8, 5.5 Hz, 2H), 3.28–2.93 (m, 2H), 1.60 (s, 9H). ^{13}C NMR (50 MHz, $CDCl_3$) δ 173.27, 172.38, 148.58, 140.95, 136.44, 135.10, 128.97, 128.32, 126.68, 124.97, 99.74, 55.40, 27.73, 23.92, 13.06, 10.47.ESI-MS (+) Calc. for $[C_{23}H_{28}ClN_3O_4]$ 445.94, found: 468.8 $[M+Na]^+$.

tert-Butyl ((S)-1-(((2S,3R)-1-amino-3-(benzyloxy)-1-oxobutan-2-yl)amino)-1-oxo-3-phenylpropan-2-yl)carbamate (34). Yield 88%. Yellowish solid. R_f = 0.8 (ethyl acetate). Mp. 161–163 ˚C. ^{1}H NMR (200 MHz, $CDCl_3$) δ 7.38–7.26 (m, 7H), 7.10–7.06 (m, 2H), 6.63 (s br, 1H), 6.39 (s br, 1H), 5.65 (s br, 1H), 5.08 (s br, 1H), 4.81–4.77 (m, 1H), 4.38–4.35 (m, 1H), 3.15–2.97 (m, 5H), 1.74–1.47 (m, 3H), 1.41 (s, 9H). ^{13}C NMR (50 MHz, $CDCl_3$) δ 172.98, 171.90, 156.38, 137.70, 136.53, 128.99, 128.42, 128.13, 127.64, 127.58, 126.75, 80.30, 74.03, 71.36, 60.44, 38.05, 27.67, 20.33, 15.75. ESI-MS (+) Calc. for $[C_{25}H_{33}N_3O_5]$ 455.55, found: 478.5 $[M+Na]^+$.

tert-Butyl ((S)-1-(((2R,3S)-1-amino-3-(benzyloxy)-1-oxobutan-2-yl)amino)-1-oxo-3-phenylpropan-2-yl)carbamate (35). Yield 78%. Yellowish solid. R_f = 0.8 (ethyl acetate). Mp. 138–139 ˚C. ^{1}H NMR (200 MHz, $CDCl_3$) δ 7.40–7.37 (m, 7H), 7.11–7.08 (m, 2H), 6.58 (s br, 1H), 6.43 (s br, 1H), 5.61 (s br, 1H), 5.23 (s br, 1H), 4.83–4.78 (m, 1H), 4.34–4.31 (m, 1H), 3.32–2.85 (m, 5H), 1.39 (s, 9H), 1.19–1.09 m, 3H). ^{13}C NMR (50 MHz, $CDCl_3$) δ 173.34, 172.27, 156.74, 138.07, 136.90, 129.35, 128.79, 128.49, 128.01, 127.95, 127.12, 80.66, 74.40, 71.73, 60.81, 38.42, 28.04, 20.70, 16.12.ESI-MS (+) Calc. for $[C_{25}H_{33}N_3O_5]$ 455.55, found: 478.5 $[M+Na]^+$.

tert-Butyl ((S)-1-(((2S,3R)-1-amino-3-(benzyloxy)-1-oxobutan-2-yl)amino)-4-methyl-1-oxopentan-2-yl)carbamate (36). Yield 76%. Yellowish solid. R_f = 0.8 (ethyl acetate). Mp. 88–91 ˚C. ^{1}H NMR (200 MHz, $CDCl_3$) δ 7.30–7.22 (m, 5H), 7.19–7.15 (m, 1H), 6.24 (s br, 1H), 6.04 (s br, 1H), 5.36 (s br, 2H), 4.57 (s, 2H), 4.56–4.52 (m, 1H), 4.36–4.21 (m, 1H), 4.17–4.11 (m, 1H), 1.77–1.48 (m, 3H), 1.38 (s, 9H), 1.13 (d, *J* = 6.4 Hz, 3H), 0.94–0.90 (m, 6H). ^{13}C NMR (50 MHz, $CDCl_3$) δ 172.84, 171.86, 155.98, 137.88, 128.29, 127.66, 127.63, 80.38, 73.89, 71.58, 56.40, 54.01, 40.85, 28.12, 24.74, 22.92, 21.62. ESI-MS (+) Calc. for $[C_{22}H_{35}N_3O_5]$ 421.53, found: 444.7 $[M+Na]^+$.

tert-Butyl ((S)-1-(((2R,3S)-1-amino-3-(benzyloxy)-1-oxobutan-2-yl)amino)-4-methyl-1-oxopentan-2-yl)carbamate (37). Yield 73%. Yellowish solid. R_f = 0.8 (ethyl acetate). Mp. 86–88 ˚C. ^{1}H NMR (200 MHz, $CDCl_3$) δ 7.31–7.22 (m, 5H), 7.20–7.11 (m, 1H), 6.26 (s br, 1H), 6.02 (s br, 1H), 5.36 (s br, 2H), 4.54 (s, 2H), 4.56–4.53 (m, 1H), 4.33–4.28 (m, 1H), 4.16–4.11 (m, 1H), 1.76–1.48 (m, 3H), 1.48 (s, 9H), 1.11 (d, *J* = 6.4 Hz, 3H), 0.96–0.90 (m, 6H). ^{13}C NMR (50 MHz, $CDCl_3$) δ 172.84, 171.86, 155.98, 137.88, 128.29, 127.66, 127.63, 80.38, 73.89, 71.58, 56.40, 54.01, 40.85, 28.12, 24.74, 22.92, 21.62. ESI-MS (+) Calc. for $[C_{22}H_{35}N_3O_5]$ 421.53, found: 444.5 $[M+Na]^+$.

tert-Butyl ((S)-1-(((2S,3R)-1-amino-3-(benzyloxy)-1-oxobutan-2-yl)amino)-3-(3-chlorophenyl)-1-oxopropan-2-yl)carbamate (38). Yield 77%. Yellowish solid. R_f = 0.6 (ethyl acetate). Mp. 164–165 ˚C. ^{1}H NMR (200 MHz, CD_3OD) δ 7.47–7.22 (m, 9H), 4.55–4.37 (m, 1H), 4.29–4.17 (m, 2H), 3.26 (dd, *J* = 13.9, 5.1 Hz, 1H), 3.07–2.96 (m, 1H), 2.92 (s, 2H), 1.44 (s, 9H), 1.27 (d, *J* = 6.3 Hz, 3H). ^{13}C NMR (50 MHz, CD_3OD) δ 172.84, 171.76, 156.24, 138.90, 137.56, 136.39,130.04, 128.85, 128.28, 127.99, 127.50, 127.44, 126.61, 80.16, 73.89, 71.22, 60.30, 49.00, 37.92, 27.53, 20.19. ESI-MS (+) Calc. for $[C_{25}H_{32}ClN_3O_5]$ 489.99, found: 513.1 $[M+Na]^+$.

Synthesis of compounds 39–49. Compounds **39**–**49** have been synthesized in two steps from their precursors **28**–**38**. After removal of the Boc-protecting group (method B), the free amine was coupled to the carboxylic acid following the general procedure for amide synthesis (method C).

N-((S)-1-(((S)-1-Amino-1-oxo-3-phenylpropan-2-yl)amino)-1-oxo-3-phenylpropan-2-yl)-3-(tert-butyl)-1-methyl-1H-pyrazole-5-carboxamide (39). Yield 79%. Yellowish solid. R_f = 0.3 (ethyl acetate). Mp. 109–110 ˚C. ^{1}H NMR (200 MHz, $CDCl_3$) δ7.32–6.96 (m, 10H), .6.65 (s br, 1H), 6.26 (s, 1H), 6.09 (s br, 1H), 4.68–4.58 (m, 2H), 3.81 (s, 3H), 2.87–2.74 (m, 4H), 1.11 (s, 9H). ^{13}C NMR (50 MHz, $CDCl_3$) δ 173.37, 165.56, 162.46, 160.20, 159.99, 136.34, 136.16, 134.40, 129.13, 128.39, 126.87, 126.81, 124.46, 103.30, 54.93, 53.91, 38.44, 36.34, 31.69, 31.28, 30.27. ESI-MS (+) Calc. for [$C_{27}H_{33}N_5O_3$] 475.58, found: 498.7 [M+Na]$^+$.

N-((S)-1-(((R)-1-Amino-1-oxo-3-phenylpropan-2-yl)amino)-1-oxo-3-phenylpropan-2-yl)-3-(tert-butyl)-1-methyl-1H-pyrazole-5-carboxamide (40). Yield 72%. Yellowish solid. R_f = 0.4 (ethyl acetate). Mp. 121–122 ˚C. ^{1}H NMR (200 MHz, $CDCl_3$) δ 7.59–7.13 (m, 10H), 6.88 (s, 1H), 6.50 (s, 1H), 6.32 (s br, 1H), 4.92–4.82 (m, 2H), 4.04 (s, 3H), 3.10–2.91 (m, 4H), 1.34 (s, 9H). ^{13}C NMR (50 MHz, $CDCl_3$) δ 172.94, 165.13, 162.04, 159.77, 159.56, 135.92, 135.74, 133.97, 128.70, 127.97, 126.45, 126.38, 124.04, 102.88, 54.50, 53.48, 38.01, 35.91, 31.26, 30.86, 29.84. ESI-MS (+) Calc. for [$C_{27}H_{33}N_5O_3$] 475.58, found: 498.7 [M+Na]$^+$.

N-((S)-1-(((S)-1-Amino-4-methyl-1-oxopentan-2-yl)amino)-1-oxo-3-phenylpropan-2-yl)-3-(tert-butyl)-1-methyl-1H-pyrazole-5-carboxamide (41). Yield 85%. Yellowish solid. R_f = 0.3 (ethyl acetate). Mp. 152–153 ˚C. ^{1}H-NMR (200 MHz, $CDCl_3$) δ. 7.42–7.25 (m, 5H), 6.81 (s, 1H), 4.77–4.65 (m, 1H), 4.36–4.08 (m, 1H), 4.08 (s, 3H), 3.22–3.18 (m, 2H), 1.89–1.46 (m, 3H), 1.40 (s, 9H), 0.88–0.80 (m, 6H). ^{13}C NMR (50 MHz, $CDCl_3$) δ 173.57, 168.11, 162.00, 161.25, 137.23, 135.94, 130.02, 129.31, 127.64, 104.97, 57.07, 49.00, 38.87, 32.59, 31.75, 30.78, 24.80, 23.57, 21.42. ESI-MS (+) Calc. for [$C_{24}H_{35}N_5O_3$] 441.57, found: 464.5 [M+Na]$^+$.

N-((S)-1-(((S)-1-Amino-3-(3-chlorophenyl)-1-oxopropan-2-yl)amino)-1-oxo-3-phenylpropan-2-yl)-3-(tert-butyl)-1-methyl-1H-pyrazole-5-carboxamide (42). Yield 72%. Yellowish solid. R_f = 0.3 (ethyl acetate). Mp. 131–133 ˚C. ^{1}H NMR (200 MHz, $CDCl_3$) δ 7.45–7.28 (s, 5H), 6.83 (s, 1H), 4.87–4.68 (m, 1H), 4.39–4.11 (m, 1H), 4.11 (s, 3H), 3.25–3.21 (m, 2H), 1.76–1.49 (m, 3H), 1.42 (s, 9H), 0.88–0.83 (m, 6H). ^{13}C NMR (50 MHz, $CDCl_3$) δ 176.49, 171.02, 164.92, 164.17, 140.15, 138.86, 132.94, 132.23, 130.56, 107.89, 76.35, 59.99, 41.79, 35.51, 34.67, 33.70, 27.72, 26.49, 24.34. ESI-MS (+) Calc. for [$C_{24}H_{35}N_5O_3$] 441.57, found: 464.5 [M+Na]$^+$.

tert-Butyl ((S)-1-(((S)-1-amino-3-(3-chlorophenyl)-1-oxopropan-2-yl)amino)-1-oxo-3-phenylpropan-2-yl)carbamate (43). Yield 80%. Yellowish solid. R_f = 0.2 (ethyl acetate). Mp. 101–103 ˚C. ^{1}H NMR (200 MHz, $CDCl_3$:CD_3OD 10:1) δ. 7.58–6.99 (m, 9H), 6.47 (s, 1H), 4.77–4.62 (m, 2H), 4.04 (s, 3H), 3.39–2.91 (m, 4H), 1.34 (s, 9H). ^{13}C NMR (50 MHz, $CDCl_3$:CD_3OD 10:1) δ 172.23, 172.21, 161.25, 161.03, 137.40, 136.96, 135.83, 135.15, 130.68, 129.87, 129.23, 128.42, 128.30, 127.69, 117.62, 104.55, 55.12, 49.00, 42.41, 38.76, 38.62, 32.51, 30.78. ESI-MS (+) Calc. for [$C_{27}H_{32}ClN_5O_3$] 510.03, found: 532.9 [M+Na]$^+$.

N-((S)-1-(((S)-1-Amino-1-oxo-3-(pyridin-4-yl)propan-2-yl)amino)-1-oxo-3-phenylpropan-2-yl)-3-(tert-butyl)-1-methyl-1H-pyrazole-5-carboxamide (44). Yield 66%. Yellowish oil. R_f = 0.2 (ethyl acetate). ^{1}H NMR (200 MHz, $CDCl_3$) δ 8.63 (d, J = 5.7 Hz, 2H), 7.58–7.30 (m, 7H), 7.36–7.13 (m, 7H), 6.59 (s, 1H), 4.84–4.68 (m, 2H), 3.89 (s, 3H), 3.35–3.07 (m, 2H), 1.27 (s, 9H) .^{13}C NMR (50 MHz, $CDCl_3$) δ 174.42, 173.04, 161.51, 161.12, 149.40, 148.81, 138.04, 136.11, 129.86, 129.09, 127.45, 126.03, 104.55, 55.73, 54.08, 38.35, 37.93, 37.75, 32.45, 30.45. ESI-MS (+) Calc. for [$C_{26}H_{32}N_6O_3$] 476.57, found:477.3 [M+H]$^+$.

N-((S)-1-(((2S,3R)-1-Amino-3-(benzyloxy)-1-oxobutan-2-yl)amino)-1-oxo-3-phenylpropan-2-yl)-3-(tert-butyl)-1-methyl-1H-pyrazole-5-carboxamide (45). Yield 65%.

Yellowish solid. R_f = 0.3 (ethyl acetate). Mp 109–110 ˚C. ^{1}H NMR (200 MHz, $CDCl_3$) δ 7.30–7.08 (m, 9H), 6.40 (d, *J* = 14.4 Hz, 1H), 6.26 (s, 1H), 5.00–4.76 (m, 1H), 4.52 (s, 2H), 4.17–4.06 (m, 2H), 3.98 (s, 3H), 3.20–3.09 (m, 2H), 1.27 (s, 9H), 1.11 (d, *J* = 6.2 Hz, 3H). ^{13}C NMR (50 MHz, $CDCl_3$) δ 171.79, 171.19, 160.58, 160.20, 137.80, 136.25, 134.62, 129.26, 128.78, 128.44, 127.84, 127.78, 127.21, 103.32, 74.00, 71.58, 60.39, 56.64, 38.86, 38.61, 31.91, 30.49, 21.02. ESI-MS (+) Calc. for [$C_{29}H_{37}N_5O_4$] 519.64, found:549.4 [M+Na]$^+$.

N-((S)-1-(((2R,3S)-1-Amino-3-(benzyloxy)-1-oxobutan-2-yl)amino)-1-oxo-3-phenylpropan-2-yl)-3-(tert-butyl)-1-methyl-1H-pyrazole-5-carboxamide (46). Yield 61%. Yellowish solid. R_f = 0.3 (ethyl acetate). Mp 119–120 ˚C. ^{1}H NMR (200 MHz, $CDCl_3$) δ.7.27–7.04 (m, 9H), 6.37 (d, *J* = 14.4 Hz, 1H), 6.22 (s, 1H), 4.97–4.73 (m, 1H), 4.48 (s, 2H), 4.14–4.03 (m, 2H), 3.95 (s, 3H), 3.17–3.06 (dd, *J* = 11.3, 5.1 Hz, 2H), 1.23 (s, 9H), 1.08 (d, *J* = 6.2 Hz, 3H). ^{13}C NMR (50 MHz, $CDCl_3$) δ 171.79, 171.19, 160.58, 160.20, 137.80, 136.25, 134.62, 129.26, 128.78, 128.44, 127.84, 127.78, 127.21, 103.32, 74.00, 71.58, 60.39, 56.64, 38.86, 38.61, 31.91, 30.49, 21.02. ESI-MS (+) Calc. for [$C_{29}H_{37}N_5O_4$] 519.64, found: 549.4 [M+Na]$^+$.

N-((S)-1-(((2S,3R)-1-Amino-3-(benzyloxy)-1-oxobutan-2-yl)amino)-4-methyl-1-oxopentan-2-yl)-3-(tert-butyl)-1-methyl-1H3-pyrazole-5-carboxamide (47). Yield 73%. Yellowish solid. R_f = 0.3 (ethyl acetate). Mp 177–178 ˚C. ^{1}H NMR (200 MHz, $CDCl_3$) δ. 7.27–7.20 (m, 4H), 7.14 (d, *J* = 8.5 Hz, 1H), 6.42 (s, 1H), 4.85–4.82 (m, 1H), 4.62–4.52 (s, 2H), 3.96 (s, 3H), 3.87–3.84 (m, 1H), 1.69–1.59 (m, 3H), 1.22 (s, 9H). 1.18 (d, *J* = 6.3 Hz, 3H), 0.90 (d, *J* = 6.0 Hz, 3H), 0.97 (d, *J* = 6.0 Hz, 3H). ^{13}C NMR (50 MHz, $CDCl_3$) δ 172.35, 171.66, 160.37, 160.31, 137.82, 134.69, 128.57, 128.00, 127.74, 103.21, 74.07, 71.71, 56.24, 52.12, 39.03, 38.69, 32.02, 30.59, 25.00, 23.01, 22.0. ESI-MS (+) Calc. for [$C_{26}H_{39}N_5O_4$] 485.62, found: 508.5 [M+Na]$^+$.

N-((S)-1-(((2R,3S)-1-Amino-3-(benzyloxy)-1-oxobutan-2-yl)amino)-4-methyl-1-oxopentan-2-yl)-3-(tert-butyl)-1-methyl-1H3-pyrazole-5-carboxamide (48). Yield 70%. Yellowish solid. R_f = 0.3 (ethyl acetate). Mp 170–171 ˚C. ^{1}H NMR (200 MHz, $CDCl_3$) δ 7.33–7.21 (m, 4H), 7.15 (d, *J* = 8.5 Hz, 1H), 6.34 (s, 1H), 4.85–4.82 (m, 1H), 4.64–4.53 (s, 2H), 3.98 (s, 3H), 3.88–3.86 (m, 1H), 1.71–1.60 (m, 3H), 1.24 (s, 9H), 1.21 (d, *J* = 6.3 Hz, 3H), 0.91 (d, *J* = 6.0 Hz, 3H), 0.89 (d, *J* = 6.0 Hz, 3H). ^{13}C NMR (50 MHz, $CDCl_3$) δ 171.72, 171.02, 159.73, 159.68, 137.18, 134.05, 127.94, 127.36, 127.10, 102.58, 73.43, 71.08, 55.60, 51.49, 38.39, 38.06, 31.39, 29.95, 24.37, 22.38, 21.44. ESI-MS (+) Calc. for [$C_{26}H_{39}N_5O_4$] 485.62, found: 508.5 [M+Na]$^+$.

N-((S)-1-(((2S,3R)-1-Amino-3-(benzyloxy)-1-oxobutan-2-yl)amino)-3-(3-chlorophenyl)-1-oxopropan-2-yl)-3-(tert-butyl)-1-methyl-1H-pyrazole-5-carboxamide (49). Yield 65%. Yellowish solid. R_f = 0.2 (ethyl acetate). Mp 102–104 ˚C. ^{1}H NMR (200 MHz, CD_3OD) δ 8.59 (d, *J* = 7.8 Hz, 1H), 8.03 (d, *J* = 8.4 Hz, 1H), 7.26 (dd, *J* = 5.6, 2.2 Hz, 9H), 6.59 (s, 1H), 4.64–4.45 (m, 3H), 4.16–4.11 (m, 1H), 3.86 (s, 3H), 3.27–3.25 (m, 1H), 3.03 (dd, *J* = 14.7, 10.8 Hz, 1H), 1.28 (s, 9H), 1.22 (d, *J* = 6.3 Hz, 3H). ^{13}C NMR (50 MHz, CD_3OD) δ 174.44, 173.31, 162.05, 161.35, 140.90, 139.31, 136.28, 134.96, 130.78, 130.33, 129.08, 128.62, 128.52, 128.44, 127.71, 104.84, 75.78, 72.24, 58.45, 55.77, 38.46, 37.34, 32.66, 30.66, 16.58. ESI-MS (+) Calc. for [$C_{29}H_{36}ClN_5O_4$] 554.08, found: 577.1 [M+Na]$^+$.

Synthesis of compounds 50–60. Compounds **50–60** have been synthesized by dehydration of the corresponding primary amide precursor **39–49** with cyanuric chloride (method A).

3-(tert-Butyl)-N-((S)-1-(((S)-1-cyano-2-phenylethyl)amino)-1-oxo-3-phenylpropan-2-yl)-1-methyl-1H-pyrazole-5-carboxamide (50). Yield 89%. Yellowish solid. R_f = 0.6 (ethyl acetate: *n*-hexane; 6:4). Mp. 89–90 ˚C. ^{1}H NMR (400 MHz, $CDCl_3$) δ 7.32–7.21 (m, 8H), 7.16 (dd, *J* = 6.4, 2.8 Hz, 2H), 6.90 (d, *J* = 8.2 Hz, 1H), 6.82 (d, *J* = 8.2 Hz, 1H), 6.35 (s, 1H), 5.04–5.02 (m, 1H), 4.82–4.80 (m, 1H), 4.02 (s, 3H), 3.21–3.07 (m, 2H), 3.00–2.98 (m, 2H), 1.33–1.30 (m, 9H). ^{13}C NMR (100 MHz, $CDCl_3$) δ 170.30, 160.25, 160.30, 135.55, 134.04, 133.37, 129.08,

129.04, 128.75, 128.72, 127.71, 127.26, 117.25, 103.06, 54.17, 41.48, 38.77, 38.35, 37.95, 31.75, 30.26. FT-IR (KBr, cm^{-1}) 3300.81, 2951.21, 2909.60, 2243.70, 1677.69, 1648.55, 1544.51, 1278.15, 1232.37, 986.82, 751.92, 670.52, 524.68, 424.97. HRMS (+) Calc. for $[C_{27}H_{32}N_5O_2]^+$ 458.25560, found: 458.2586 $[M+H]^+$. HPLC (protocol A): t_R (min) = 9.07. Purity 99.0%.

3-(tert-Butyl)-N-((S)-1-(((R)-1-cyano-2-phenylethyl)amino)-1-oxo-3-phenylpropan-2-yl)-1-methyl-1H-pyrazole-5-carboxamide (51). Yield 92%. Yellowish solid. R_f = 0.6 (ethyl acetate: *n*-hexane; 6:4). Mp. 98–99 ˚C. ^{1}H NMR (200 MHz, $CDCl_3$) δ 7.34–7.12 (m, 9H), 6.91 (d, *J* = 7.9 Hz, 1H), 6.34 (s, 1H), 5.09–5.05 (m, 1H), 4.94–4.91 (m, 1H), 4.00 (s, 3H), 3.12 (dd, *J* = 13.8, 6.4 Hz, 2H), 2.98 (dd, *J* = 13.8, 6.4 Hz, 2H), 1.30 (s, 9H). ^{13}C NMR (50 MHz, $CDCl_3$) δ 170.75, 160.43, 160.33, 135.98, 134.32, 133.78, 129.42, 129.33, 129.01, 128.86, 127.99, 127.42, 118.87, 103.48, 54.38, 41.82, 38.96, 38.48, 38.26, 31.98, 30.51. FT-IR (KBr, cm^{-1}) 3350.28, 3256.30, 2953.92, 2165.27, 1638.14, 1511.6, 1307.15, 1160.05, 1086.49, 906.70, 820.89, 694.21, 669.69, 543.02. HRMS (+) Calc. for $[C_{27}H_{32}N_5O_2]^+$ 458.25560, found: 458.2586 $[M+H]^+$. HPLC (protocol A): t_R (min) = 17.32. Purity 99.3%.

3-(tert-Butyl)-N-((S)-1-(((S)-1-cyano-3-methylbutyl)amino)-1-oxo-3-phenylpropan-2-yl)-1-methyl-1H-pyrazole-5-carboxamide (52). Yield 84%. Yellowish solid. R_f = 0.7 (ethyl acetate: *n*-hexane; 6:4). Mp 81–82 ˚C. ^{1}H NMR (200 MHz, CD_3OD) δ 7.29–7.20 (m, 5H), 6.64 (s, 1H), 4.80–4.69 (m, 2H), 3.90 (s, 3H), 3.23–2.94 (m, 2H), 1.78–1.62 (m, 3H), 1.27 (s, 9H), 0.95–0.91 (m, 6H). ^{13}C NMR (50 MHz, CD_3OD) δ 173.33, 161.87, 161.51, 138.07, 136.59, 130.36, 129.56, 127.93, 119.68, 105.02, 56.04, 49.00, 42.00, 40.04, 38.69, 32.86, 30.88, 25.80, 22.35, 22.19. FT-IR (KBr, cm^{-1}) 3403.41, 3309.42, 3203.18, 2953.92, 2937.57, 1695.35, 1634.05, 1523.72, 1368.44, 1274.46, 1245.86, 1168.22, 835.58, 702.38, 669.69, 567.54. HRMS (+) Calc. for $[C_{24}H_{34}N_5O_2]^+$ 423.27125, found: 424.27572 $[M+H]^+$. HPLC (protocol A): t_R (min) = 9.16. Purity 97.4%.

3-(tert-Butyl)-N-((S)-1-(((S)-1-cyano-3-methylbutyl)amino)-1-oxo-3-phenylpropan-2-yl)-1-methyl-1H-pyrazole-5-carboxamide (53). Yield 79%. White solid. R_f = 0.7 (ethyl Acetate: *n*-hexane; 6:4). Mp. 91–94 ˚C. ^{1}H NMR (200 MHz, $CDCl_3$) δ 7.32–7.21 (m, 3H), 6.98 (d, *J* = 8.2 Hz, 1H), 6.88 (d, *J* = 8.2 Hz, 1H), 6.34 (s, 1H), 4.92–4.86 (m, 1H), 4.77–4.71 (m, 1H), 3.99 (s, 3H), 3.29–3.19 (m, 2H), 1.63–1.46 (m, 3H), 1.27 (s, 9H), 0.88 (2d, *J* = 5.9 Hz, 6H). ^{13}C NMR (50 MHz, $CDCl_3$) δ 171.28, 161.15, 161.04, 136.68, 135.04, 129.97, 129.56, 128.05, 119.17, 104.16, 55.16, 41.95, 39.62, 39.12, 32.67, 31.19, 25.31, 22.79, 22.53. FT-IR (KBr, cm^{-1}) 3350.28, 3256.30, 2953.92, 2165.27, 1638.14, 1511.46, 1307.15, 1160.05, 1086.49, 906.70, 820.89, 694.21, 669.69, 543.02. HRMS (+) Calc. for $[C_{24}H_{34}N_5O_2]^+$ 423.27125, found: 424.27572 $[M+H]^+$. HPLC (protocol A): t_R (min) = 9.42. Purity 99.1%.

3-(tert-Butyl)-N-((S)-1-(((S)-2-(3-chlorophenyl)-1-cyanoethyl)amino)-1-oxo-3-phenylpropan-2-yl)-1-methyl-1H-pyrazole-5-carboxamide (54). Yield 50%. Yellowish solid. R_f = 0.6 (ethyl acetate: *n*-hexane; 6:4). Mp 132–133 ˚C. ^{1}H NMR (200 MHz, CD_3OD/ $CDCl_3$) δ 7.54–7.35 (m, 9H), 6.75 (s, 1H), 5.19–5.11 (m, 1H), 4.51–4.48 (m, 1H), 4.17 (s, 3H), 3.33–3.21 (m, 4H), 1.49 (s, 9H). ^{13}C NMR (50 MHz, CD_3OD) δ 172.23, 161.25, 161.03, 137.40, 136.96, 135.83, 135.15, 130.68, 130.07, 129.87, 129.23, 128.42, 128.30, 127.69, 118.18, 104.55, 55.12, 42.41, 38.76, 38.62, 32.51, 30.78. FT-IR (cm^{-1}) 3288.99, 2925.31, 2855.85, 2161.18, 1666.74, 1634.05, 1544.15, 1507.38, 1450.17, 1266.29, 1221.34, 1074.23, 861.75, 747.33, 706.47, 694.21. HRMS (+) Calc. for $[C_{27}H_{31}ClN_5O_2]^+$ 491.21663, found: 492.21034 $[M+H]^+$. HPLC (protocol A): t_R (min) = 9.61. Purity > 99.9%.

3-(tert-Butyl)-N-((S)-1-(((S)-1-cyano-2-(pyridin-4-yl)ethyl)amino)-1-oxo-3-phenylpropan-2-yl)-1-methyl-1H-pyrazole-5-carboxamide (55). Yield 35%. Yellowish wax. *R* = 0.4 (ethyl acetate: *n*-hexane; 6:4). ^{1}H NMR (400 MHz, CD_3OD) δ 8.44 (s br, 2H), 7.38 (d, *J* = 5.3 Hz, 2H), 7.30–7.22 (m, 5H), 6.63 (s, 1H), 5.14 (t, *J* = 7.5 Hz, 1H), 4.66 (dd, *J* = 8.6, 6.8 Hz, 1H), 3.94 (s, 3H), 3.26–3.13 (m, 4H), 1.30 (s, 9H). ^{13}C NMR (100 MHz, DMSO-d_6) δ 171.17, 170.90, 159.29, 158.46, 137.89, 136.81, 135.23, 134.81, 129.27, 128.86, 128.13, 127.92, 126.93, 126.34,

118.94, 60.46, 53.87, 53.24, 41.15, 31.39, 30.18, 13.74. FT-IR (cm^{-1}) 3264.47, 2953.92, 2913.05, 2851.76, 2161.43, 1662.66, 1605.45, 1548.24, 1466.62, 1204.99, 1115.10, 996.59, 800.45, 735.07, 681.95. HRMS (+) Calc. for $[C_{26}H_{31}N_6O_2]^+$ 459.25085, found: 459.25627 $[M+H]^+$. HPLC (protocol A): t_R (min) = 6.84. Purity 98.6%.

N-((S)-1-(((1R,2R)-2-(Benzyloxy)-1-cyanopropyl)amino)-1-oxo-3-phenylpropan-2-yl)-3-(tert-butyl)-1-methyl-1H-pyrazole-5-carboxamide (56). Yield 80%. White solid. R_f = 0.5 (ethyl acetate: *n*-hexane; 6:4). Mp. 115–116 ˚C. ^{1}H-NMR (200 MHz, $CDCl_3$) δ 7.35–7.26 (m, 10H), 6.95 (d, *J* = 8.7 Hz, 1H), 6.61 (d, *J* = 7.0 Hz, 1H), 6.30 (s, 1H), 4.88–4.85 (m, 2H), 4.62–4.58 (m, 1H), 4.03 (s, 3H), 3.82–3. 78 (m, 1H), 3.29–3.24 (m, 2H), 1.31 (s, 9H), 1.03 (d, *J* = 6.0 Hz, 3H). ^{13}C NMR (50 MHz, $CDCl_3$) δ 170.30, 159.83, 159.62, 136.42, 135.27, 133.75, 128.67, 128.41, 128.00, 127.60, 127.30, 126.87, 116.63, 102.65, 72.60, 70.91, 53.85, 44.51, 38.33, 37.60, 31.40, 29.94, 15.29. FT-IR (cm^{-1}) 3354.37, 3252.21, 2181.61, 1654.61, 1654.48, 1540.07, 1486.95, 1290.81, 1151.87, 1086.48, 894.44, 808.63, 710.56, 661.32, 543.02. HRMS (+) Calc. for $[C_{29}H_{36}N_5O_3]^+$ 502.28182, found: 502.28095 $[M+H]^+$. HPLC (protocol A): t_R (min) = 9.54. Purity 99.4%.

N-((S)-1-(((1S,2S)-2-(Benzyloxy)-1-cyanopropyl)amino)-1-oxo-3-phenylpropan-2-yl)-3-(tert-butyl)-1-methyl-1H-pyrazole-5-carboxamide (57). Yield 82%. White solid. R_f = 0.5 (ethyl acetate: *n*-hexane; 6:4). Mp. 123–124 ˚C. ^{1}H NMR (200 MHz, $CDCl_3$) δ 7.36–7.25 (m, 10H), 6.98 (d, *J* = 8.7 Hz, 1H), 6.65 (d, *J* = 7.0 Hz, 1H), 6.32 (s, 1H), 4.91–4.83 (m, 2H), 4.63–4.60 (m, 1H), 4.05 (s, 3H), 3.80 (s br, 1H), 3.24–3.20 (m, 2H), 1.33 (s, 9H), 1.05 (d, *J* = 6.0 Hz, 3H). ^{13}C NMR (50 MHz, $CDCl_3$) δ 171.01, 160.54, 160.34, 137.14, 135.98, 134.46, 129.39, 129.12, 128.71, 128.32, 128.02, 127.59, 117.34, 103.37, 72.85, 71.15, 54.56, 45.22, 39.04, 38.32, 32.12, 30.65, 16.00. FT-IR (cm^{-1}) 2376.73, 2958.00, 2169.35, 1642.22, 15400.07, 1499.21, 1442.00, 1290.81, 1225.43, 1111.01, 1033.37, 988.42, 743.25, 690.12. HRMS (+) Calc. for $[C_{29}H_{36}N_5O_3]^+$ 502.28182, found: 502.28095 $[M+H]^+$. HPLC (protocol A): t_R (min) = 9.43. Purity 98.3%.

N-((S)-1-(((1R,2R)-2-(Benzyloxy)-1-cyanopropyl)amino)-4-methyl-1-oxopentan-2-yl)-3-(tert-butyl)-1-methyl-1H-pyrazole-5-carboxamide (58). Yield 78%. White solid. R_f = 0.5 (ethyl acetate: *n*-hexane; 6:4). Mp. 96–97 ˚C. ^{1}H NMR (400 MHz, DMSO-d_6) δ 8.93 (d, *J* = 8.1 Hz, 1H), 8.43 (d, *J* = 7.6 Hz, 1H), 7.38–7.29 (m, 5H), 6.88 (s, 1H), 5.07–5.04 (m, 1H), 4.64–4.61 (m, 2H), 4.59–4.56 (m, 1H), 3.97–3.94 (m, 3H), 3.86–3.84 (m, 1H), 1.72–1.64 (m, 2H), 1.50–1.46 (m, 2H), 1.26–1.20 (m, 12H), 0.93 (d, *J* = 6.3 Hz, 3H), 0.88 (d, *J* = 6.5 Hz, 3H). ^{13}C NMR (100 MHz, DMSO-d_6) δ 172.36, 159.56, 158.66, 137.92, 134.92, 128.10, 127.53, 127.45, 117.82, 103.73, 73.39, 70.40, 51.05, 44.75, 38.44, 31.53, 30.31, 24.25, 22.91, 21.19, 15.69. FT-IR (cm^{-1}) 3378.89, 3350.28, 3186.83, 2958.00, 2116.43, 1674.91, 1650.40, 1531.90, 1368.44, 1262.20, 1160.05, 1057.89, 1033.37, 780.02, 735.07, 649.26, 604.31. HRMS (+) Calc. for $[C_{26}H_{38}N_5O_3]$ 468.29746, found: 468.29785 $[M+H]^+$. HPLC (protocol A): t_R (min) = 9.61. Purity 98.3%.

N-((S)-1-(((1S,2S)-2-(Benzyloxy)-1-cyanopropyl)amino)-4-methyl-1-oxopentan-2-yl)-3-(tert-butyl)-1-methyl-1H-pyrazole-5-carboxamide (59). Yield 70%. White solid. R_f = 0.5 (ethyl acetate: *n*-hexane; 6:4). Mp. 110–111 ˚C. ^{1}H NMR (400 MHz, $CDCl_3$) δ 7.27–7.20 (m, 5H), 7.14 (d, *J* = 8.5 Hz, 1H), 6.42 (d, *J* = 7.8 Hz, 1H), 6.33 (s, 1H), 4.85–4.82 (m, 1H), 4.62–4.52 (m, 3H), 3.96 (s, 3H), 3.87–3.84 (m, 1H), 1.69–1.59 (m, 3H), 1.22 (s, 9H). 1.18 (d, *J* = 6.3 Hz, 3H) 1.24–1.19 (m, 12H), 0.92–0.88 (m, 6H). ^{13}C NMR (100 MHz, $CDCl_3$) δ 172.10, 160.65, 160.51, 137.21, 134.43, 128.66, 128.23, 127.92, 117.45, 103.16, 73.69, 71.80, 51.75, 45.28, 40.81, 38.06, 32.10, 30.62, 25.04, 22.97, 22.13, 16.36. FT-IR (cm^{-1}) 3333.94, 3284.90, 2962.09, 2868.10, 2255.16, 1647.44, 1540.07, 1507.38, 1442.00, 1274.46, 1245.86, 988.42, 739.16, 661.52. HRMS (+) Calc. for $[C_{26}H_{38}N_5O_3]$ 468.29746, found: 468.29785 $[M+H]^+$. HPLC (protocol A): t_R (min) = 9.56. Purity 96.9%.

N-((S)-1-(((1R,2R)-2-(Benzyloxy)-1-cyanopropyl)amino)-3-(3-chlorophenyl)-1-oxopropan-2-yl)-3-(tert-butyl)-1-methyl-1H-pyrazole-5-carboxamide (60). Yield 50%. Yellowish wax. R_f = 0.4 (ethyl acetate: *n*-hexane; 6:4). ^{1}H NMR (400 MHz, $CDCl_3$) δ 7.30–7.13 (m, 6H), 7.04 (dt, *J* = 7.0, 1.7 Hz, 1H), 6.62 (dd, *J* = 17.8, 8.2 Hz, 2H), 6.25 (s, 1H), 4.77–4.71 (m, 2H), 4.48 (dd, *J* = 36.1, 11.7 Hz, 2H), 3.95 (s, 3H), 3.82–3.74 (m, 1H), 3.11–3.00 (m, 2H), 1.20 (s, 9H), 1.08 (d, *J* = 6.3 Hz, 3H). ^{13}C NMR (100 MHz, $CDCl_3$) δ 170.73, 160.54, 160.12, 137.80, 136.91, 134.84, 134.30, 130.44, 129.51, 128.71, 128.34, 128.03, 127.84, 127.62, 117.06, 103.35, 73.35, 71.72, 54.28, 45.07, 39.06, 38.13, 32.07, 30.58, 16.21. FT-IR (cm^{-1}) 3357.24, 3264.21, 2193.15, 1654.33, 1538.29, 1487.88, 1209.18, 1141.78, 1036.43, 863.33, 807.36, 701.44, 658.23, 534.57. ESI-MS (+) Calc. for [$C_{29}H_{345}ClN_5O_3$] 536.24284, found: 536.24235 $[M+H]^+$.HPLC (protocol B): t_R (min) = 12.06. Purity 96.5%.

Synthesis of compounds 61–64. Compounds **61–64** have been synthesized from compounds **34–37** by removal of the benzyl group through hydrogenation on Pd/C (method A).

N-((S)-1-(((2S,3R)-1-Amino-3-hydroxy-1-oxobutan-2-yl)amino)-1-oxo-3-phenylpropan-2-yl)-3-(tert-butyl)-1-methyl-1H-pyrazole-5-carboxamide.(61). Yield 92%. Colorless wax. R_f = 0.2 (ethyl acetate). ^{1}H NMR (200 MHz, $CDCl_3$) δ 8.03 (s, 1H), 7.36–6.94 (m, 5H), 6.54 (s, 1H), 4.44–4.39 (m, 2H), 4.03–4.01 (m, 1H), 3.96 (s, 3H), 3.18–3.14 (m, 1H), 2.87 (s, 1H), 1.30 (s, 9H), 1.03–1.01 (m, 3H). ^{13}C NMR (50 MHz, $CDCl_3$) δ 173.54, 172.15, 161.25, 160.35, 136.25, 135.98, 134.58, 129.36, 128.76, 127.25, 66.60, 58.51, 55.55, 54.30, 38.70, 31.98, 30.51, 18.92. ESI-MS (+) Calc. for [$C_{22}H_{31}N_5O_4$] 429.51, found:452.4 $[M+Na]^+$.

N-((S)-1-(((2R,3S)-1-Amino-3-hydroxy-1-oxobutan-2-yl)amino)-1-oxo-3-phenylpropan-2-yl)-3-(tert-butyl)-1-methyl-1H-pyrazole-5-carboxamide.(62). Yield 95%. Colorless wax. R_f = 0.2 (ethyl acetate). ^{1}H NMR (200 MHz, $CDCl_3$) δ 8.01 (s, 1H), 7.36–6.98 (m, 5H), 6.59 (s, 1H), 4.42–4.36 (m, 2H), 4.04–4.01 (m, 1H), 3.96 (s, 3H), 3.12–3.09 (m, 1H), 2.89 (s, 1H), 1.33 (s, 9H), 1.03–0.99 (m, 3H). ^{13}C NMR (50 MHz, $CDCl_3$) δ 173.54, 172.15, 161.25, 160.35, 136.25, 135.98, 134.58, 129.36, 128.76, 127.25, 66.60, 58.51, 55.55, 54.30, 38.70, 31.98, 30.51, 18.92. ESI-MS (+) Calc. for [$C_{22}H_{31}N_5O_4$] 429.51, found: 452.4 $[M+Na]^+$.

N-((S)-1-(((2S,3R)-1-Amino-3-hydroxy-1-oxobutan-2-yl)amino)-4-methyl-1-oxopentan-2-yl)-3-(tert-butyl)-1-methyl-1H-pyrazole-5-carboxamide(63). Yield 90%. Colorless wax. R_f = 0.2 (ethyl acetate). ^{1}H NMR (200 MHz, $CDCl_3$) δ 7.37 (d, *J* = 3.9 Hz, 1H), 6.74–6.71 (m, 2H), 6.42 (s, 1H), 4.71–4.68 (m, 1H), 4.42–4.38 (m, 2H), 4.06 (s, 3H), 1.71–1.68 (m, 3H), 1.27 (s, 9H), 1.14–1.11 (m, 3H), 0.98–0.92 (m, 6H). ESI-MS (+) Calc. for [$C_{19}H_{33}N_5O_4$] 395.51, found: 418.5 $[M+Na]^+$.

N-((S)-1-(((2R,3S)-1-Amino-3-hydroxy-1-oxobutan-2-yl)amino)-4-methyl-1-oxopentan-2-yl)-3-(tert-butyl)-1-methyl-1H-pyrazole-5-carboxamide (64). Yield 93%. Colorless wax. R_f = 0.2 (ethyl acetate). ^{1}H NMR (200 MHz, $CDCl_3$) δ 7.34 (d, *J* = 3.9 Hz, 1H), 6.79–6.75 (m, 2H), 6.46 (s, 1H), 4.73–4.70(m, 1H), 4.45–4.41 (m, 2H), 4.11 (s, 3H), 1.77–1.74 (m, 3H), 1.28 (s, 9H), 1.19–1.17 (m, 3H), 0.99–0.91 (m, 6H). ESI-MS (+) Calc. for [$C_{19}H_{33}N_5O_4$] 395.51, found: 418.5 $[M+Na]^+$.

Synthesis of compounds 65–68. Compounds **65–68** have been synthesized by dehydration of the corresponding primary amide precursor **61–64** with trifluoroacetic anhydride (method B).

3-(tert-Butyl)-N-((S)-1-(((1R,2R)-1-cyano-2-hydroxypropyl)amino)-1-oxo-3-phenylpropan-2-yl)-1-methyl-1H-pyrazole-5-carboxamide (65). Yield 45%. White solid. R_f = 0.7 (ethyl acetate). Mp. 159–160 °C. ^{1}H NMR (500 MHz, $CDCl_3$) δ 7.32–7.26 (m, 4H), 7.26–7.21 (m, 1H), 6.65 (s, 1H), 4.84–4.79 (m, 2H), 3.96 (s, 3H), 3.88–3.84 (m, 1H), 3.20 (dd, *J* = 13.6, 7.1 Hz, 1H), 3.10 (dd, *J* = 13.6, 7.1 Hz, 1H), 1.31 (s, 9H), 1.07 (d, *J* = 6.3 Hz, 3H). ^{13}C NMR (125 MHz, $CDCl_3$) δ 173.35, 162.06, 161.60, 138.15, 136.69, 130.42, 129.57, 127.98, 118.24, 105.04, 67.67, 56.05, 38.86, 38.68, 32.90, 30.87, 18.89, 18.55. FT-IR (KBr, cm^{-1}) 3293.08, 2953.92,

2913.05, 2868.10, 1646.10, 1540.07, 1446.08, 1286.72, 1237.68, 1098.75, 922.51, 739.16, 689.30, 469.47. HRMS (+) Calc. for $[C_{22}H_{30}N_5O_3]^+$ 412.23486, found: 412.23811 $[M+H]^+$. HPLC (protocol A): t_R (min) = 7.65. Purity 97.8%.

3-(tert-Butyl)-N-((S)-1-(((1S,2S)-1-cyano-2-hydroxypropyl)amino)-1-oxo-3-phenylpropan-2-yl)-1-methyl-1H-pyrazole-5-carboxamide (66). Yield 42%. White solid. R_f = 0.7 (ethyl acetate). Mp. 145–147 ˚C. ^{1}H NMR (400 MHz, $CDCl_3$) δ 7.31–7.23 (m, 5H), 7.07 (d, *J* = 8.0 Hz, 1H), 6.67 (d, *J* = 7.5 Hz, 1H), 6.31 (s, 1H), 4.85–4.84 (m, 1H), 4.72–4.68 (m, 1H), 4.15–4.10 (m, 1H), 4.02 (s, 3H), 3.21–3.15 (m, 2H), 1.29–1.27 (m, 9H), 1.08 (d, *J* = 6.2 Hz, 3H). ^{13}C NMR (100 MHz, $CDCl_3$) δ 172.41, 171.26, 160.58, 135.89, 134.27, 129.38, 129.14, 127.65, 117.25, 103.52, 67.39, 54.76, 47.02, 39.11, 38.38, 32.09, 30.59, 19.02. FT-IR (KBr, cm^{-1}) 3289.11, 2955.43, 2918.55, 2860.11, 1649.54, 1543.16, 1444.02, 1277.62, 1233.66, 1091.87, 944.77, 745.55, 690.34, 477.11. HRMS (+) Calc. for $[C_{22}H_{30}N_5O_3]^+$ 412.23486, found: 412.23811 $[M+H]^+$.HPLC (protocol A): t_R (min) = 7.71. Purity 95.7%.

3-(tert-Butyl)-N-((S)-1-(((1R,2R)-1-cyano-2-hydroxypropyl)amino)-4-methyl-1-oxopentan-2-yl)-1-methyl-1H-pyrazole-5-carboxamide (67). Yield 33%. White solid. R_f = 0.5 (ethyl acetate). Mp. 118–119 ˚C. ^{1}H NMR (400 MHz, $CDCl_3$) δ 7.56–7.51 (m, 1H), 6.80–6.75 (m, 1H), 6.43 (s, 1H), 4.87–4.83 (m, 1H), 4.65–4.63 (m, 1H), 4.15–4.11 (m, 1H), 4.06 (s, 3H), 1.31–1.20 (m, 15H), 0.97 (2d, *J* = 6.2 Hz, 3H). ^{13}C NMR (100 MHz, $CDCl_3$) δ 174.32, 161.62, 162.14, 135.77, 117.22, 104.56, 67.34, 52.68, 41.12, 38.28, 31.46, 32.15, 26.11, 23.56, 21.65, 19.03. FT-IR (KBr, cm^{-1}) 3297.16, 2953.92, 2913.05, 2868.10, 1646.31, 1535.89, 1503.29, 1462.52, 1364.36, 1282.63, 1172.38, 1131.44, 996.59, 730.99, 592.05. HRMS (+) Calc. for $[C_{19}H_{32}N_5O_3]^+$ 378.25071, found: 378.25231 $[M+H]^+$.HPLC (protocol A): t_R (min) = 8.08. Purity: 96.7%.

3-(tert-Butyl)-N-((S)-1-(((1S,2S)-1-cyano-2-hydroxypropyl)amino)-4-methyl-1-oxopentan-2-yl)-1-methyl-1H-pyrazole-5-carboxamide (68). Yield 35%. White solid. R_f = 0.5 (ethyl acetate). Mp. 111–113 ˚C. ^{1}H NMR (400 MHz, CD_3OD) δ 6.78 (s, 1H), 4.88–4.84 (m, 1H), 4.65–4.60 (m, 1H), 4.07–4.05 (m, 1H), 4.05 (s, 3H), 1.81–1.61 (m, 4H), 1.32 (s, 9H), 1.26 (d, *J* = 6.3 Hz, 3H), 1.00 (2d, *J* = 6.3 Hz, 6H). ^{13}C NMR (100 MHz,CD_3OD) δ 175.01, 162.46, 161.76, 136.76, 118.59, 105.26, 68.00, 53.28, 41.76, 39.00, 33.07, 31.04, 26.27, 23.54, 21.94, 19.44. FT-IR (KBr, cm^{-1}) 3293.08, 2962.09, 2917.14, 2847.67, 1646.31, 1540.07, 1458.34, 1278.55, 1131.44, 1078.32, 1000.68, 853.58, 812.71, 780.02, 730.99, 559.36. HRMS (+) Calc. for $[C_{19}H_{32}N_5O_3]^+$ 378.25071, found: 378.25231 $[M+H]^+$. HPLC (protocol A): t_R (min) = 7.94. Purity: 98.6%.

Synthesis of compound 69. Compound **69** has been synthesized by removal of the benzyl group from compound **60** with DDQ (method B).

3-(tert-butyl)-N-((S)-3-(3-chlorophenyl)-1-(((1R,2R)-1-cyano-2-hydroxypropyl) amino)-1-oxopropan-2-yl)-1-methyl-1H-pyrazole-5-carboxamide (69). Yield 32%. White solid. R_f = 0.3 (ethyl acetate). Mp. 102–103 ˚C. ^{1}H NMR (400 MHz, CD_3OD) δ 7.35–7.28 (m, 4H), 6.69 (s, 1H), 4.87–4.83 (m, 2H), 3.99 (s, 3H), 3.90–3.84 (m, 1H), 3.24 (dd, *J* = 13.6, 7.1 Hz, 1H), 3.08 (dd, *J* = 13.6, 6.5 Hz, 1H), 1.34 (s, 9H), 1.11 (d, *J* = 6.3 Hz, 3H). ^{13}C NMR (100 MHz, CD_3OD) δ 175.23, 163.23, 151.94, 151.48, 128.04, 126.57, 120.30, 120.10, 119.52, 119.45, 117.86, 108.12, 94.92, 57.55, 45.93, 28.74, 28.56, 22.78, 20.75, 18.78. FT-IR (KBr, cm^{-1}) 3284.90, 3056.07, 2958.00, 2925.31, 2868.10, 1638.14, 1556.41, 1499.21, 1462.43, 1364.36, 1270.37, 1229.51, 1098.75, 878.09, 730.99, 702.38, 453.12. ESI-MS (+) Calc. for $[C_{22}H_{29}ClN_5O_3]^+$ 446.19589, found: 446.19745 $[M+H]^+$.HPLC (protocol A): t_R (min) = 8.55. Purity 99.7%.

Enzyme inhibition studies

Enzyme inhibition studies for Cz and LmCPB were performed as previously described for Cz [15]. The experimental procedures are described in the Supporting Information (see chapter S3). Cathepsins B, L, S were assayed as reported [18,19].

All experiments were performed in triplicate and for the most potent compounds ($pK_i >$ 7.5) two other independent experiments were performed.

Cathepsin K assay. Human recombinant cathepsin K was assayed on a FLUOSTAR Optima plate reader at 25 ˚C with an excitation wavelength of 360 nm and an emission wavelength of 440 nm on a 96 well plate. The enzyme solution (23 μg/mL in 50 mM sodium acetate pH 5.5, 50 mM NaCl, 0.5 mM EDTA, 5 mM DTT) was diluted 1:100 with assay buffer (100 mM sodium citrate buffer pH 5.0, 100 mM NaCl, 1 mM EDTA, 0.01% CHAPS) containing 5 mM DTT and was then incubated at 37 ˚C for 30 min for activation. A 1.5 mM stock solution of the substrate Z-Leu-Arg-AMC was prepared in DMSO. The final substrate concentration was 6 μM (= 3.05 × K_m). The assay was performed with a final concentration of cathepsin K of 1.73 ng/mL. Stock solutions of inhibitors were prepared in DMSO. The final DMSO concentration was 2% (4 μL). Into a well containing 194.5 μL assay buffer, 0.8 μL of the fluorogenic substrate, DMSO and inhibitor solution (3.2 μL) were added. Upon addition of cathepsin K (1.5 μL), the measurement was started and followed for 20 min.

Mammalian cytotoxicity assay

$LLCMK_2$ cells were cultured in 96-well plates at a concentration of 5 x 104 cells/ml. After 48 h, the plates were washed twice with PBS and 200 μL RPMI medium was added with serial dilutions of the compounds and benznidazole (1.95 μM to 250 μM) in triplicate. After 72 h at 37 ˚C, the cytotoxic activity of the compounds was determined by the classical MTT [3-(4,5-dimethylthiazol-2-yl) -2,5-diphenyltetrazolium bromide] method. Briefly, 50 μL MTT dissolved in PBS (2.0 mg mL^{-1}) was added to each well and the plates were incubated for 4 h at 37 ˚C. The formed formazan crystals were dissolved with DMSO (50 μL/well) and the absorbance of the samples was measured by spectrophotometer at 570 nm after 30 min. The cytotoxicity results (CC_{50}) were calculated as a percentage by the formula [(ABScontrol-ABSample / ABS control) * 100], where ABScontrol represents the mean absorbance of the untreated control (viable cells) and ABSample, the absorbance of each cellular treatment.

All experiments were performed in triplicate and for the most potent compounds ($EC_{50} <$ 100) two other independent experiments were performed.

In vitro trypanocidal activity evaluation on intracellular amastigote forms (Tulahuen strain)

Cells were evaluated in 96-well plates. Cells from the $LLCMK_2$ lineage were plated at a concentration of $5x10^4$ cells mL^{-1}. Trypomastigote forms of the Tulahuen LacZ strain were added at a concentration of $5×10^5$ parasites mL^{-1} and placed in the incubator at 37˚C with 5% CO_2 for 24 h. After the incubation period, the trypomastigote forms present were removed by successive washes with PBS, remaining only as intracellular amastigote forms. Compounds were added at different concentrations (1.95 μM to 250 μM serial dilutions) and incubated for 72 h. At the end of this period, the substrate CPRG (chlorophenol red β-D-galactopyranoside, 400 μM in 0.3% Triton X-100, pH 7.4) was added. After 4 h of incubation at 37 ˚C, the plates were analyzed in a spectrophotometer at 570 nm to obtain the effective concentration (EC_{50}) to reduce the parasitemia inside the host cell. Benznidazole was used as a positive control in the same concentrations as the substances, and DMSO as a negative control. Compounds were solubilized in DMSO. The selectivity index (SI) was calculated using the formula: $SI = EC_{50}/CC_{50}$. All statistical analyses were done with the program GraphPad Prism v.5.

All experiments were performed in triplicate and for the most potent compounds ($CC_{50} <$ 100) two other independent experiments were performed.

Results

Structure-based design, modeling studies, and compound synthesis

Cz, the recombinant form of cruzipain, is a monomeric enzyme, composed of two folded and equally sized domains. These domains are divided by the enzyme's active site, which is V-shaped and primarily exposed to solvent. A catalytic triad cysteine-histidine-asparagine forms the active site [14]. The main polar interactions between the protein and inhibitor are well conserved involving the residues Gln19, Gly66, Asp161, His162, and Trp184 (residue numbers correspond to the cruzipain sequence) of the enzyme. Cz is a cathepsin L-like cysteine protease and is closely related to the mammalian CPs such as CatB, CatK, CatL, and CatS.

A variety of studies have been conducted on optimization strategies for the interactions of different classes of inhibitors with the S1, S2 and S3 binding sites of cruzain and related cysteine proteases [12,14,15,20]. Nonetheless, far less is known about the attainable interactions at S1′ for dipeptidyl nitrile inhibitors [21]. The high-resolution crystal structure of cruzain shows that there is a large open surface characterized by Trp177 in the primed binding site region (Fig 3) [22]. The design of compounds to exploit this cavity would provide enhanced enzyme-inhibitor interactions. This concept has already been applied for a class of different dipeptidic vinyl sulfone inhibitors [23]. As Fig 3 (left) exemplarily illustrates, the substituents of vinyl sulfone inhibitors predominantly sit on top of the shelf formed by residues Ser139, Met142 and Asp158 rather than adopting an orientation for an intense aromatic–aromatic interactions with Trp177. The nitrile inhibitor 33L does not bear an appropriate substituent that would allow for interaction with the primed binding region of cruzain (Fig 3, right).

The nitrile warhead has been applied successfully for a variety of series of cathepsin inhibitors. Peptidic nitriles are known to interact with the active site cysteine by forming a covalent, but reversible thioimidate adduct [24]. The nitrile warhead was also repurposed for Cz inhibition as trypanocidal agents, displaying low toxicity, probably due to the reversible character of interaction [25]. Therefore, starting from our recent study on dipeptidyl nitriles as trypanocidal agents, we expanded our previous inhibitor series to map the S1/S1′ subsites of Cz [14]. By applying a knowledge-based design approach, we have explored different amino acids as possible building blocks for the P1 moiety. Based on a template crystal structure of the dipeptidyl nitrile inhibitor 33L bound to Cz (PDB ID: 4QH6), structural modifications have been executed that might increase the affinity towards the S1' specificity pocket. Fig 4 shows dipeptidyl nitriles **50**, **52**, **56**, and **58** with different lipophilic substitution patterns at the P1 position, which were assumed to accommodate the S1′ pocket through hydrophobic interactions without interfering in the general mode of binding.

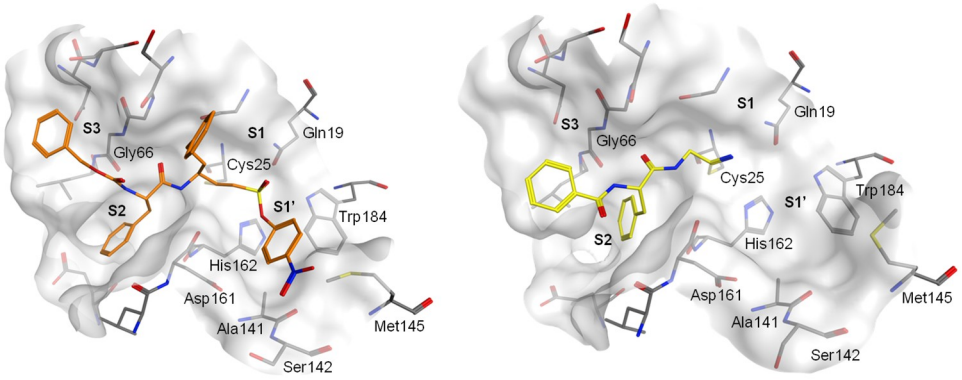

Fig 3. Crystal structures of vinyl sulfone derivative K777 and dipeptidyl nitrile 33L covalently bound to cruzain. Left. K777 in the active site of cruzain (PDB-ID: 1F2B). Right 33L in the active site of cruzain (PDB-ID 4QH6).

https://doi.org/10.1371/journal.pntd.0007755.g003

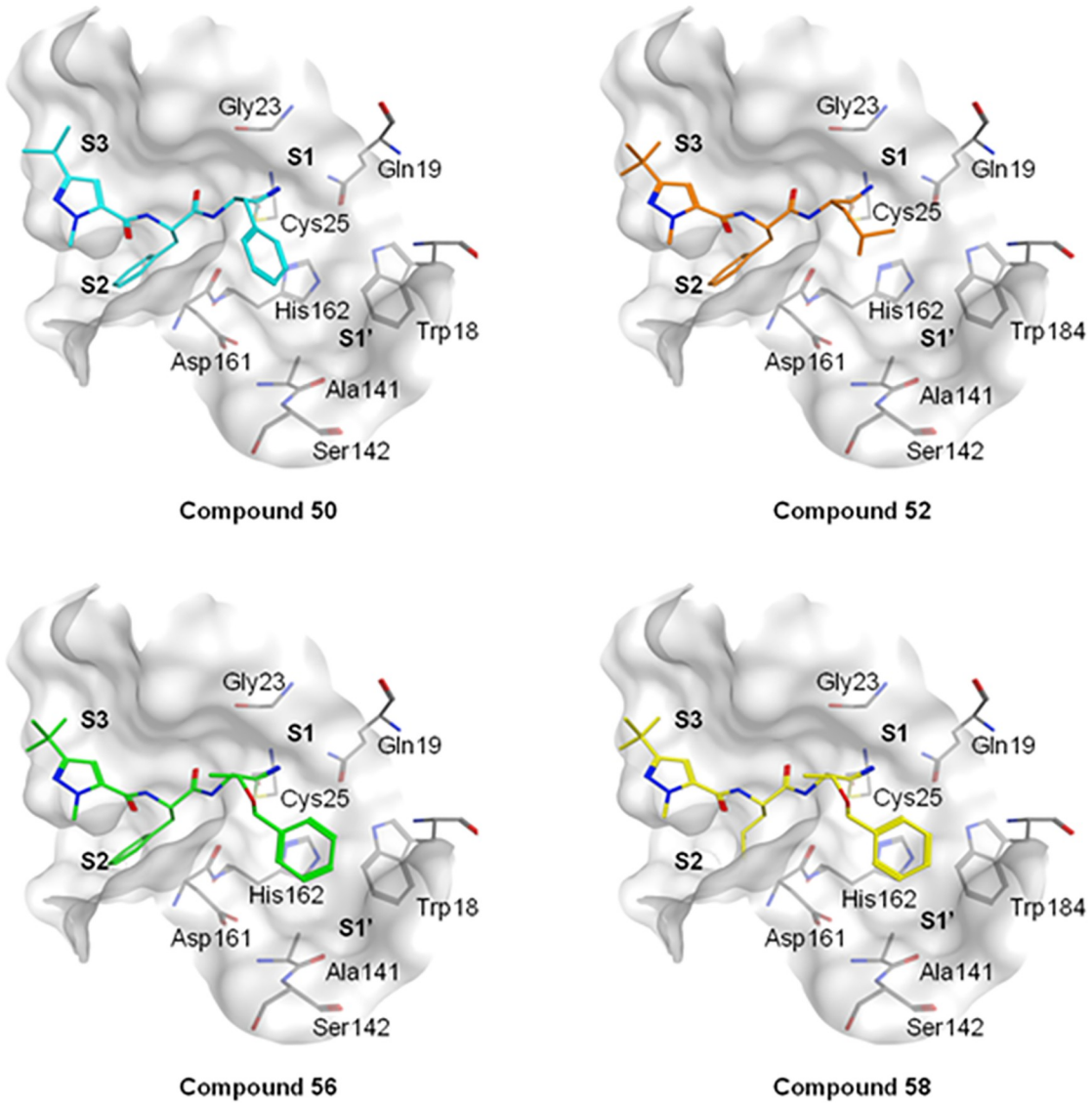

Fig 4. The putative orientation of P1 moieties in compounds 50, 52, 56, and 58.

https://doi.org/10.1371/journal.pntd.0007755.g004

Possible interactions of inhibitors with residues forming the S1 and S1' pockets of cruzain (PDB ID: 4QH6). Residue numbers are referring to the cruzipain sequence.

Compound **9** (Fig 5) was adopted as an archetype, with the cyclopropyl group at P1 position and phenylalanine in P2 as well as a pyrazole moiety in P3 for advantageous interactions with the non-primed binding region of the target protease. We mainly used different natural and unnatural amino acids for the P1 moiety and maintained the nitrile warhead. Leucine (Leu) and phenylalanine (Phe) were incorporated (compounds **50**–**54**, Fig 6) as molecular sensors in P1 for aliphatic and aromatic interactions. 4-Pyridylalanine was implemented to leverage the affinity by polar interaction with Asp161 (S1´). Thr-O-Bzl, an unusual building block for peptide inhibitors, was used as a chimera in P1 for aliphatic and aromatic interactions in the S1/S1´ area. After removal of the benzyl protecting group from Thr-O-Bzl, the so produced alcoholic moiety should allow the evaluation of whether a hydrogen bond donor is tolerated in

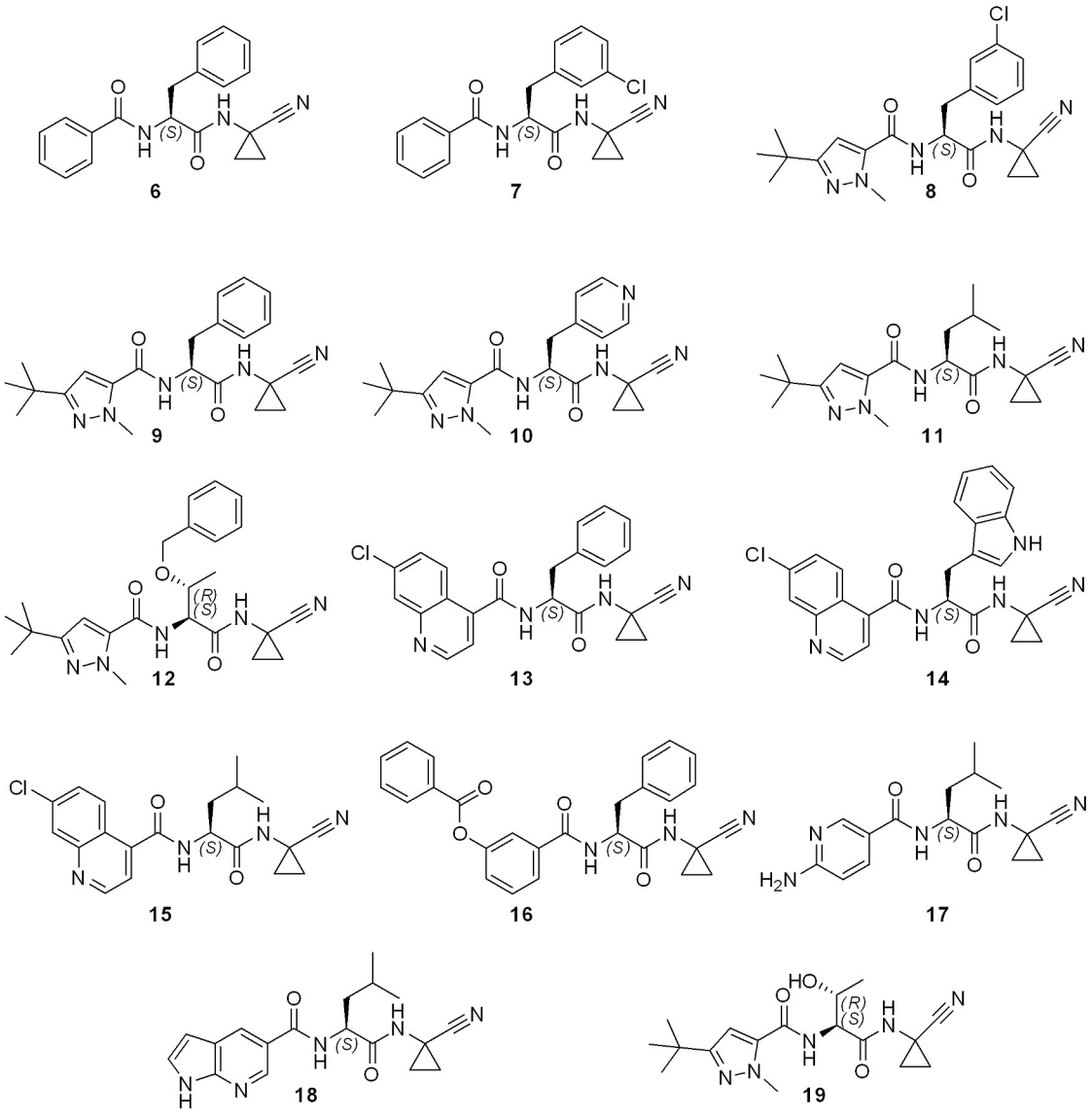

Fig 5. Structure representation of compounds 6–19.

https://doi.org/10.1371/journal.pntd.0007755.g005

the S1/S1′ area. Moreover, it was intended to investigate how the stereochemistry in this region will influence the affinity with Cz.

3-(*tert*-Butyl)-1-methyl-1*H*-pyrazole-5-carboxylic acid is a privileged building block applied for the inhibition of Cz and CatL [26]. Thus, we have explored some possible bioisosteres in order to increase the affinity and the selectivity towards Cz, such as 7-chloroquinoline carboxylic acid, 1*H*-indole-5-carboxylic acid, or 6-aminonicotinic acid.

Accordingly, we synthesized a new series of dipeptidyl nitriles (Figs 1 and 2). For compounds **6**–**12** and **14**–**19** bearing a cyclopropyl moiety in P1, the synthesis was carried out as known from the literature [15]. The peptide coupling reaction was performed twice, first to connect the enantiomerically pure, Boc-protected P2 amino acid with the aminonitrile moiety, and secondly, after removing the Boc group, to introduce the corresponding aroyl acids (Fig 1). Compound **19** was synthesized from compound **12** by removing the benzyl group under mild oxidative conditions (Fig 1) [27].

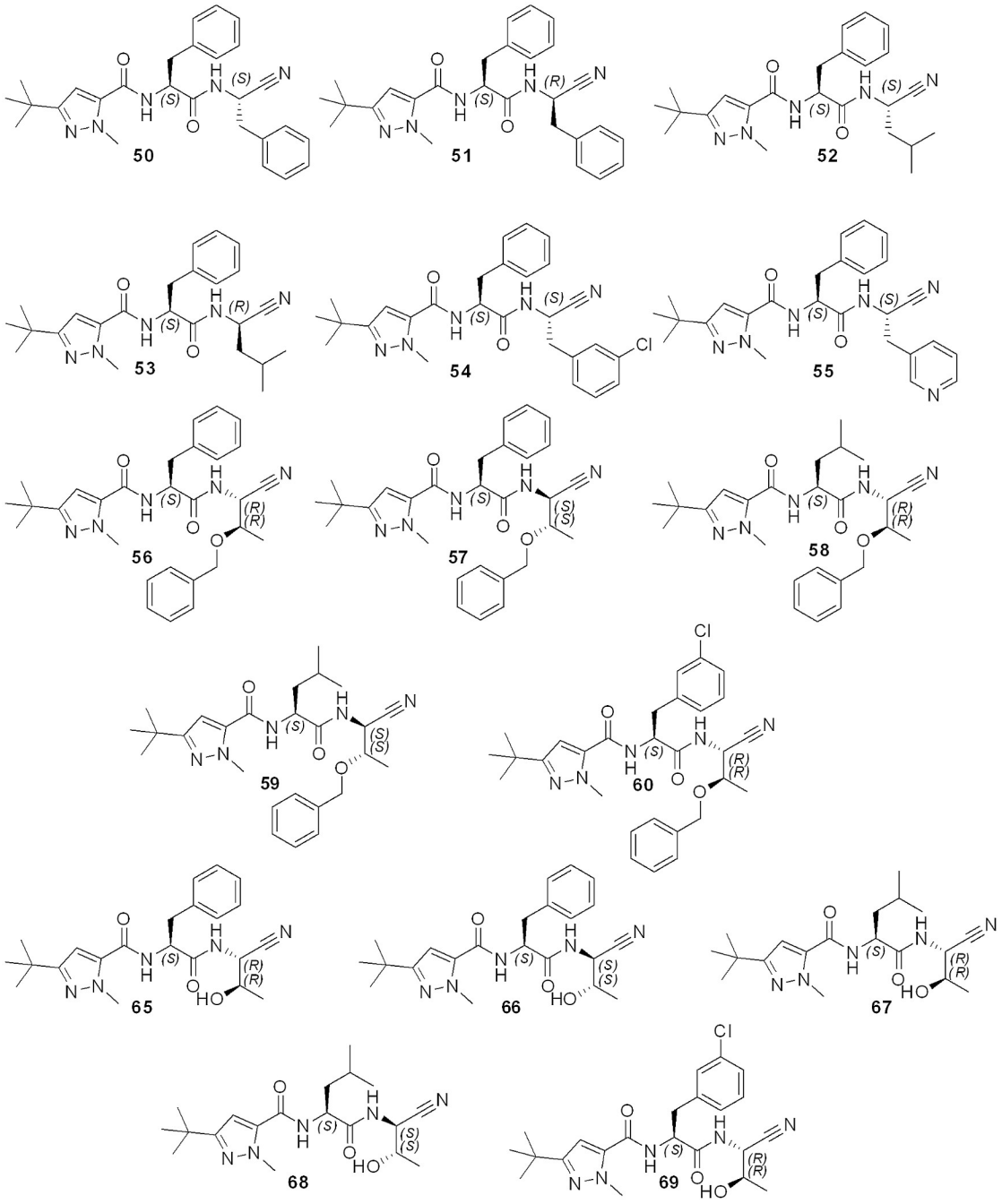

Fig 6. Structure of compounds 50–60 and 65–69.

https://doi.org/10.1371/journal.pntd.0007755.g006

For the synthesis of compounds **50–60** (Fig 6), we have adopted a different synthetic strategy. In general, the desired dipeptidyl primary amide was synthesized, followed by the dehydration reaction to form the dipeptidyl nitrile. Due to the diversity of building blocks, it was necessary to evaluate different dehydrating reagents, aiming at the best yield and prevention of racemization. For compounds **65–68** the cleavage of the benzyl group was performed by hydrogenolysis before the conversion of the primary amide to the nitrile, while for compound

69, considering the lability of the chlorine atom under hydrogenolysis, we first transformed the primary amide to the nitrile and then removed the benzyl group under mild oxidative conditions [27]. The absolute geometry of the P1 group did not change, but, owing to CIP priority rules, the configuration at the α–carbon for the Thr-O-Bzl building block changed two times: (i) in the dehydration step to form the nitrile group and, (ii) when the catalytic cysteine attacks the carbon atom of the nitrile warhead to form a covalent bond (Fig 7).

Structure-activity relationships for inhibition of cysteine proteases by dipeptidyl nitriles

The pK_i values were determined for parasite cysteine proteases (Cz, LmCPB) and also for human cysteine cathepsins (CatB, CatK, CatL, CatS) and are reported in Table 1. Compounds **6**, **8**, **9** and **11** have already been described as competitive inhibitors that bind reversibly to Cz [14]. Several new compounds are Cz nanomolar inhibitors and exhibit good affinity for LmCPB, CatL, CatS and CatK (pK_i over 7.5). The application of such inhibitors extends to candidates for antiprotozoal action and as inhibitors of cysteine cathepsins.

One crucial question is the cross-reactivity of CP inhibitors, for which an extrathermodynamic relationship can be formulated [28,29]. Ligand-target affinity involves enthalpy and entropy, which, in most cases, results in enthalpy-entropy compensation (EEC) [30]. The compensation effect should lead to an observable linear relationship between enthalpy and entropy when ligands differ by a single molecular modification. EEC is a fundamental extrathermodynamic phenomenon in medicinal chemistry and one of its grand challenges [31]. A thermodynamic analysis is commonly applied to a series of compounds that act on the same target. Here, the ligand is kept invariant while the targets are changed. Therefore, the nature of the ligand-target interaction governed by the thermodynamic parameter of the free energy change (via the estimation of the dissociation constant) results in extrathermodynamic relationships for the set of derivatives.

Hence, we investigated the degree of linear correlation between Cz and the other CPs by plotting the pK_i data against each other. The results (see S1 Fig) indicated an extrathermodynamic relationship between Cz and LmCPB, while this was not observed for all the other CPs. This finding highlights that the mode of inhibition for this series of compounds is similar for Cz and LmCPB, corroborating the fact that all the structural transformations of prototype compounds **9** and **11** affected the affinity towards the two protozoa CPs with the same magnitude (Figs 8 and 9). Therefore, known Cz inhibitors can be repurposed as LmCPB inhibitors, and the knowledge acquired in the design of Cz inhibitors can be translated into future LmCPB inhibition studies.

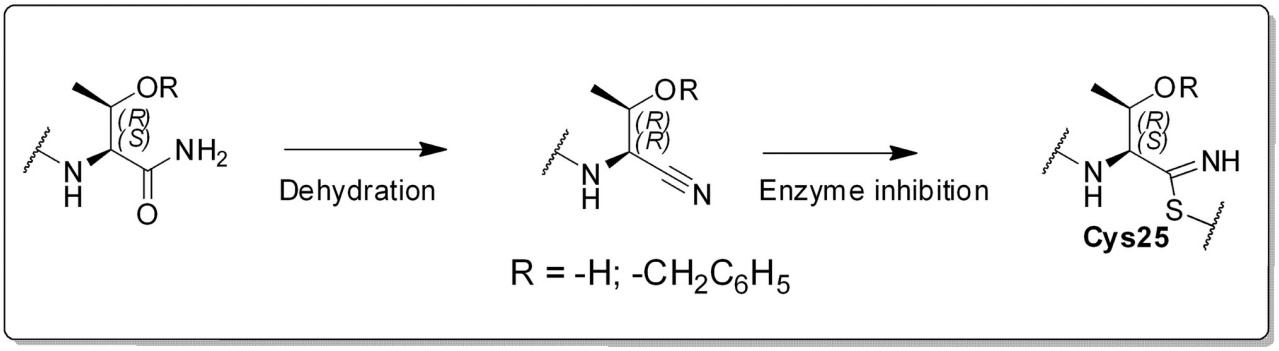

Fig 7. Change in stereochemistry for compounds bearing Thr or Thr-O-Bzl group in P1.

https://doi.org/10.1371/journal.pntd.0007755.g007

Table 1. Number identification, pK_i values for CatB, CatK, CatL, CatS, Cz and LmCPB.

	pK_i values[a] or remaining activity (%) at 10 μM[b]					
Cmpd.	**CatB**	**CatK**	**CatL**	**CatS**	**Cz**	**LmCPB**
6	73%[b]	6.4	7.4	7.1	6.6	6.6
7	5.5	6.2	7.3	7.7	6.9	6.2
8	5.4	6.4	8.6	6.7	7.4	6.7
9	4.8	6.5	8.2	6.8	7.3	7.1
10	93%[b]	5.0	7.6	5.6	6.6	6.4
11	4.5	8.3	7.6	7.4	7.8	7.3
12	4.4	96%[b]	5.9	5.9	5.1	5.5
13	4.9	81%[b]	7.2	6.7	6.7	6.9
14	4.7	n.i.[c]	5.7	6.0	6.2	5.7
15	89%[b]	6.9	6.6	6.9	7.8	7.3
16	5.2	6.2	6.3	7.3	6.9	7.0
17	n.i.[c]	8.0	6.5	7.6	7.1	6.8
18	4.5	8.7	7.1	7.3	7.7	7.2
19	4.6	5.5	5.2	5.0	51%[b]	67%[b]
50	4.5	6.3	8.5	7.3	7.7	7.8
51	94%[b]	5.6	6.9	5.9	6.3	6.1
52	5.1	6.7	8.3	6.9	7.5	7.4
53	90%[b]	6.0	7.0	6.0	6.5	6.4
54	4.9	6.3	8.3	7.1	7.5	7.5
55	4.8	6.5	8.3	7.2	7.5	7.2
56	5.2	5.7	7.0	6.0	6.3	6.5
57	n.i.[c]	97%[b]	85%[b]	n.i.[c]	75%[b]	72%[b]
58	5.1	7.8	7.2	7.3	7.9	7.7
59	n.i.[c]	n.i.[c]	90%[b]	85%[b]	60%[b]	75%[b]
60	6.3	6.0	8.1	6.5	7.2	6.8
65	92%[b]	86%[b]	5.3	5.3	68%[b]	69%[b]
66	89%[b]	81%[b]	5.6	4.7	5.4	4.8
67	92%[b]	7.8	7.0	5.0	7.1	6.7
68	93%[b]	5.1	88%[b]	83%[b]	5.4	54%[b]
69	5.2	6.1	8.2	6.6	6.9	6.0

[a] The standard deviation was lower than 15% for all reported pK_i values.

[b] Percentage of remaining activity at 10 μM, number of replicates = 2.

[c] n.i. = no inhibition observed at 10 μM.

https://doi.org/10.1371/journal.pntd.0007755.t001

One common approach to SAR analysis is to examine ΔpK_i values associated with particular structural transformations, and these can be specified concisely using the square bracket notation previously described [32]. For example, the structural transformation of the phenylalanine in P2 of compound **6** to the corresponding 3-chloro-phenylalanine (**8**) can be noted as [**6**→**8**]. As already described for Cz [14], the exchange of benzoyl by 1-methyl-3-*tert*-butyl-pyrazolyl-carbonyl [**6**→**9**] led to a potency increase of 0.5 log units. Following this path, we inserted a meta-benzoic ester in the P3 position in the attempt to design a prodrug analog [15]. The transformation [**6**→**16**] unfortunately displayed a slight increment as compared to the transformation [**6**→**13**]. Hence, compound **9** (pK_i of 7.4 for Cz) has been used as a prototype for mapping S1-P1 interaction on different targets (Fig 8).

The effects on affinity resulting from stereochemical modifications in P1 of the structural prototype **9** are shown in Fig 8. In general, the stereochemistry of P1 moiety strongly

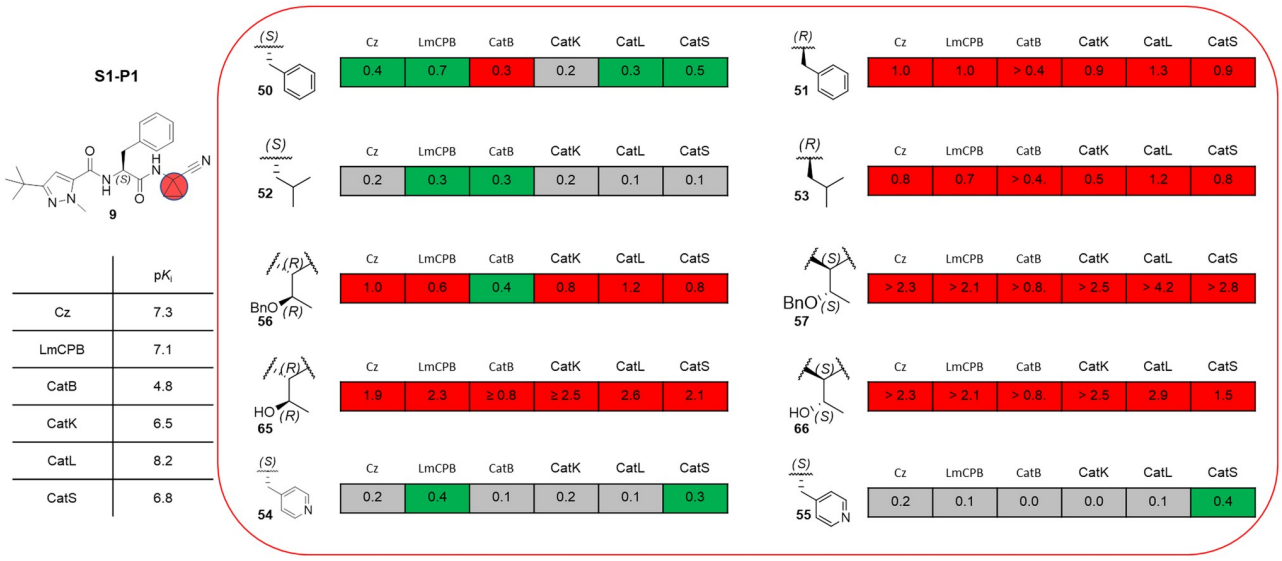

Fig 8. SAR summary for P1-S1/S1′ interactions. Values are reported as differences in pK_i and are color-coded as red (negative), green (positive), grey (no significant difference, $\Delta pK_i < 0.2$).

https://doi.org/10.1371/journal.pntd.0007755.g008

influences the affinity towards all the CPs. The (*S*) → (*R*) conversion in [**50**→**51**] and [**52**→**53**] decrease the pK_i values for Cz and LmCP both by about one log unit. Likewise, the double stereochemical modification from (*R*,*R*) benzyl-protected threonine to the (*S*,*S*) diastereomer [**56**→**57**] led to a complete all-target affinity loss. Instead, the structural transformation from the cyclopropyl unit to CH attached with a benzyl group [**9**→**50**] resulted in a significant affinity increment for Cz (pK_i of 7.7) and LmCPB (pK_i of 7.8) of 0.4 and 0.7 log units, respectively. Replacement of the P1 cyclopropane linker with CH attached to isopropyl [**9**→**52**], 3-chlorobenzyl [**9**→**54**], or even 4-pyridyl [**9**→**55**] led to a small increase or no significant difference in affinity against those two protozoa enzymes. Moreover, the insertion of the benzyl protected threonine in P1 [**9**→**56**] and [**9**→**57**] decreased the affinity for Cz and LmCPB. Remarkably, replacement by the hydroxybutyl residues led to an almost one hundredfold affinity loss for both enzymes. In general, those results are corroborated by the docking studies which display a reasonable accommodation of the aromatic and hydrophobic moieties in the S1′ site without forming any specific interaction with the residues present in this area. While, for smaller moieties as cyclopropane or Thr-OH the interaction is manly in the interface between the S1 and the S1′. Primarily, the same trend in affinity was observed for the four mammalian CPs, when the structural modifications in P1 were realized starting from the prototype compound **9**, as illustrated in Fig 8. Singularly, the introduction of a benzyl-protected threonine [**9**→**50**] resulted in a pK_i decrease of 0.3 log units towards CatB.

As recently described [14], the effects on affinity when replacing the P2 phenylalanine (**9**) with leucine (**11**) appears to depend on the substructural context, and this relates to non-additivity in the SAR. Accordingly, we used compound **11** as a starting prototype for another SAR considering P1, P2, and P3 for structural modifications, as summarized in Fig 9.

Substitution of the in P3 positioned 1-methyl-3-*tert*-butyl-pyrazole ring (**11**) with 7-chloroquinoline (**15**), or 1*H*-indole (**19**) preserved the high affinity towards Cz and LmCPB, and, strikingly, this substitution led to a decrease of 1.0 and 0.5 in the pK_i value for CatL (Fig 9). Insertion of a basic moiety, *i.e.*, 2-amino pyridine [**11**→**18**], produced a significant reduction of potency for Cz (-0.7) and LmCPB (-0.5). Compound **19** showed a high affinity for CatK

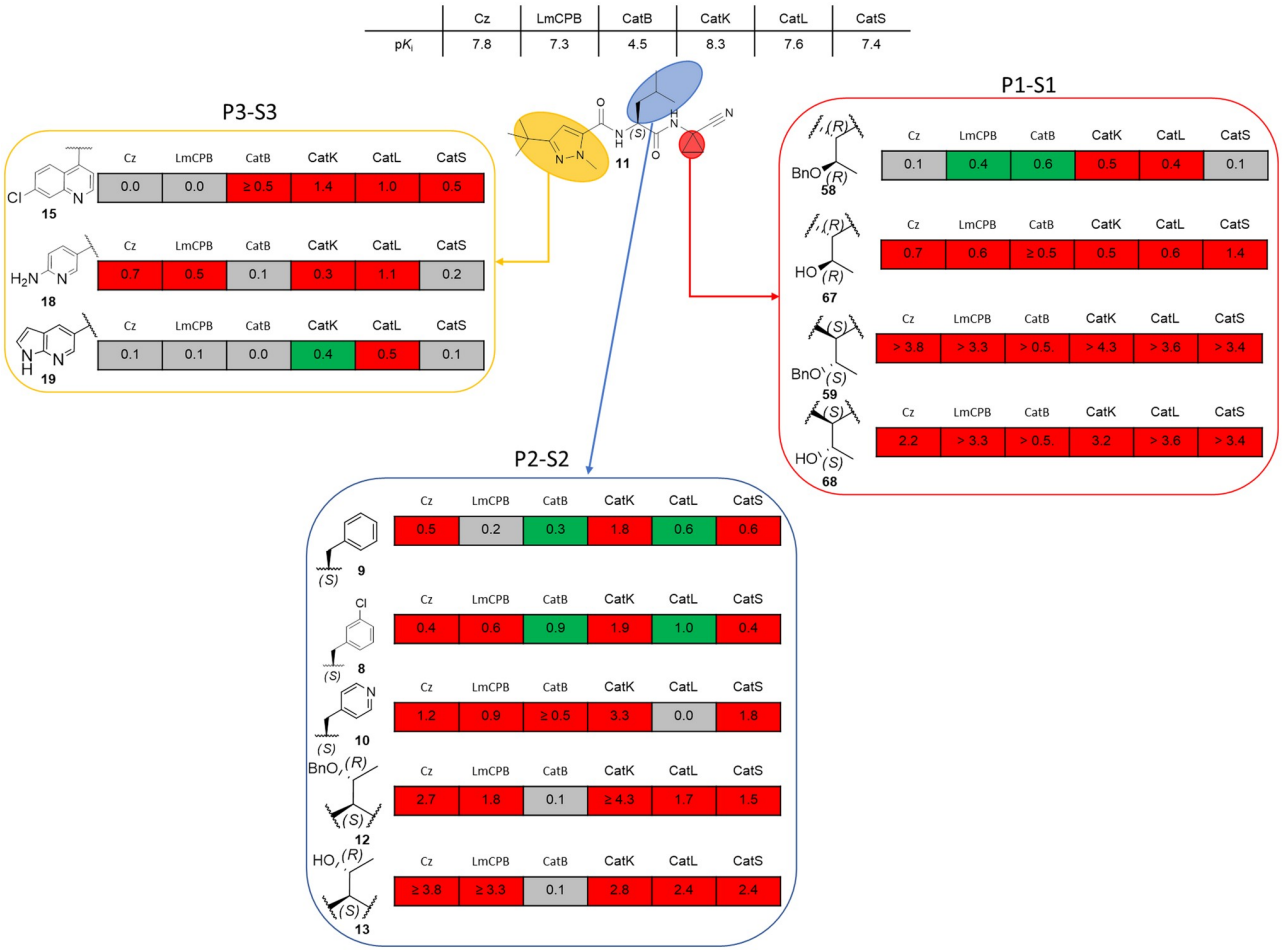

Fig 9. SAR summary starting from compound 11. Values are reported as differences in pK_i and are color-coded as red (negative), green (positive), grey (no significant difference, $\Delta pK_i < 0.2$).

https://doi.org/10.1371/journal.pntd.0007755.g009

(pK_i of 8.7) with a significant selectivity over the other mammalian CPs (Table 1). At position P2, the transformation of the leucine moiety into tryptophan, phenylalanine, or derivatives thereof resulted in an affinity loss of up to one log unit for Cz. A similar replacement led to a gain in affinity towards CatL and CatB, and it is consistent with previously reported data [33]. For compound **11**, as for compound **9**, the stereochemistry of the substituent in P1 was vitally for the bimolecular recognition process. Moreover, the transformation [**11**→**58**] kept the pK_i in the same range for Cz while increasing it by 0.4 log units for LmCPB.

Non-additivity in SAR is of considerable interest [34], and this is illustrated for the six cysteine proteases in Fig 10. Non-additivity can be quantified by comparing the ΔpK_i value resulting from a pair of substructural transformations with the sum of ΔpK_i values that result from the individual transformations. The Cz ΔpK_i values for [**9**→**11**] (0.5) and [**9**→**56**] (-1.0) shown in Fig 10A sum up to -0.5. Nevertheless, [**9**→**58**], which corresponds to the simultaneous application of the pair transformations, is associated with a ΔpK_i value increase of +0.6, thus indicating that the effects of this pair of transformations on Cz affinity are superadditive. The same was true for the effects of these two transformations on the other five CPs. Analogous analysis of the results in Fig 10B displays the effects of two transformations to be superadditive

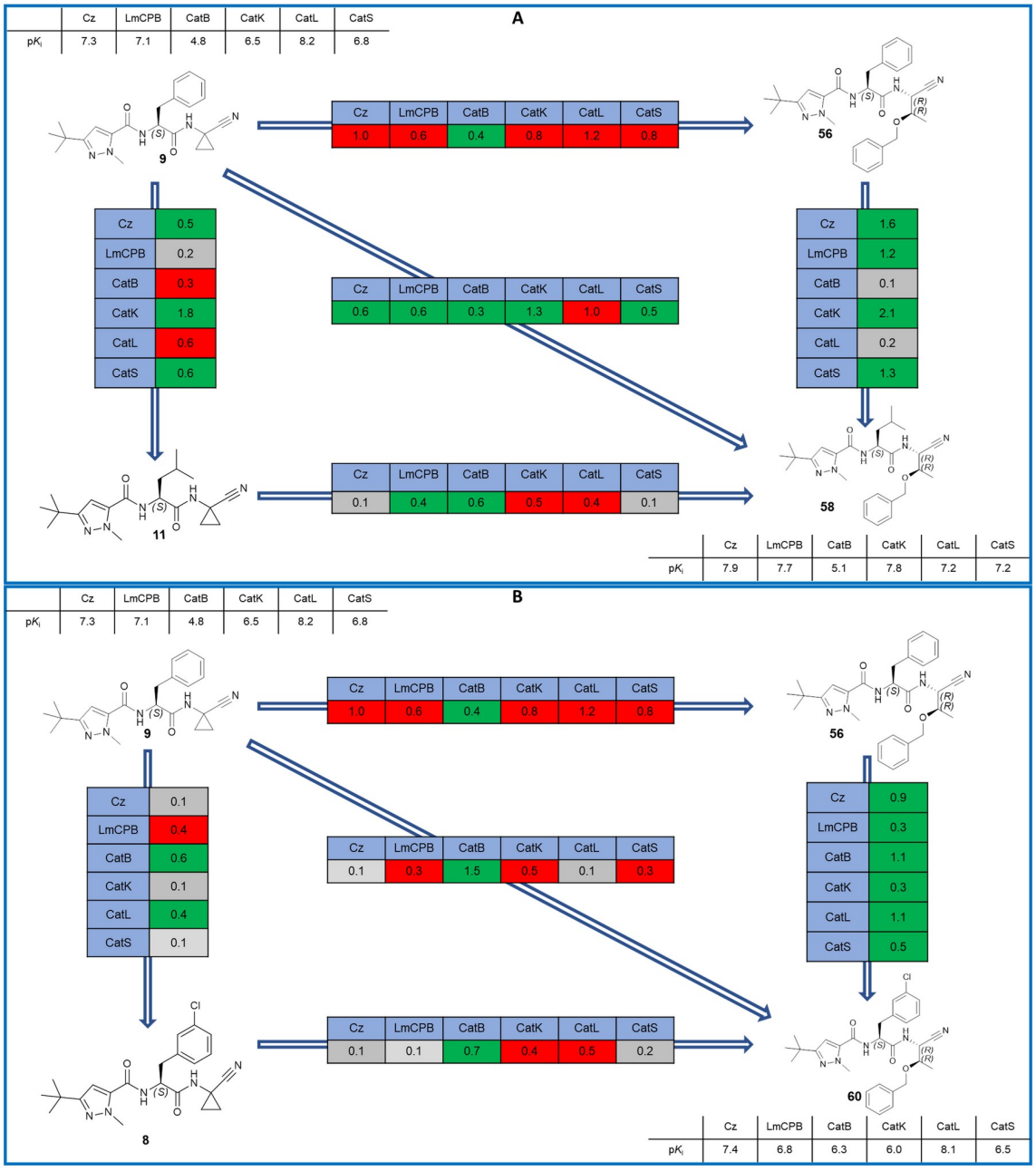

Fig 10. Non-additivity of SAR. Values are reported as differences in pK_i and are color-coded as red (negative), green (positive), grey (no significant difference, $\Delta pK_i < 0.2$).

https://doi.org/10.1371/journal.pntd.0007755.g010

for the entire CP targets investigated herein. These results entail the P1-S1 and P1'-S1' interactions to be driven by the molecular recognition in P2.

Pairwise plots for the selectivity towards Cz in relation to other human cathepsins are provided in Fig 11. It is not trivial to achieve a significant selectivity for Cz inhibitors ($\Delta pK_i > 1.0$) over mammalian CPs due to their high structural similarity of the active site. Undeniably, CatB has a different mode of binding due to the larger S2 and S3 pockets [33]. Compounds **15** (pK_i of 7.8 for Cz) and **67** (pK_i of 7.1) displayed a significant selectivity toward CatL (pK_i of

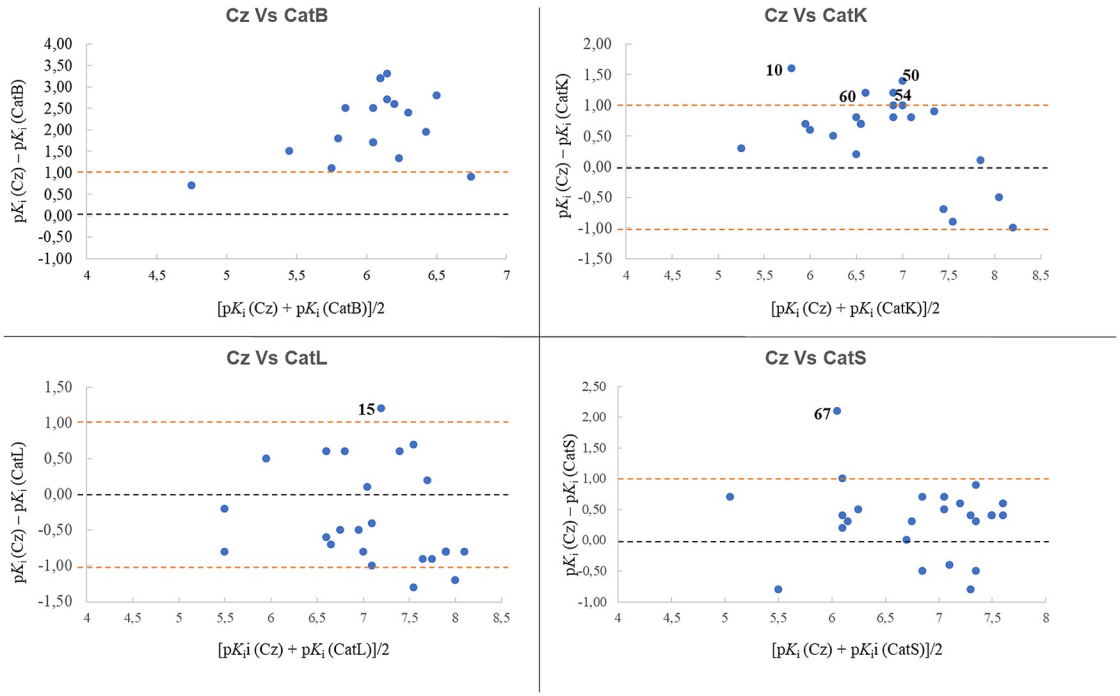

Fig 11. Selectivity pairwise plots. Values are given in pK_i. The X-axis represents the difference in pK_i for the same inhibitor for a pair of CPs. Y-axis represents the mean value of pK_i for the same inhibitor for a pair of CPs. The black dashed line highlights no selectivity. The magenta dashed line highlights a significant selectivity. Positive differences correspond to Cz pK_i values that are greater than those for CatB, CatK, CatL or CatS.

https://doi.org/10.1371/journal.pntd.0007755.g011

6.6) and CatS (pK_i of 5.0), respectively. The Cz selectivity in the case of compound **15** is driven by the S3-P3, while that of **67** is driven by S1-P1 interaction. Additionally, the hydrophobic interaction in S1 and S1´ with P1 of compounds **50** (pK_i of 7.7 for Cz), **54** (pK_i of 7.5 for Cz) and **60** (pK_i of 7.2 for Cz) resulted in a good selectivity over CatK (pK_i of 6.3, 6.3 and 6.0, respectively, for **50**, **54** and **60**). On the other hand, our study highlights two low nanomolar inhibitors of mammalian CPs: compounds **8** (pK_i of 8.6 for CatL) and **19** (pK_i of 8.7 for CatK) which showed an affinity difference of more than one log unit compared to the other mammalian cathepsins.

Biological evaluation

All compounds synthesized were evaluated for their trypanocidal activity against the amastigote form of the Tulahuen *T. cruzi* strain, and the best results are presented in Table 2. A number of 15 compounds had pEC_{50} values above 4 against *T. cruzi* amastigotes and three (**52**, **57** and **60**) were equipotent to the gold standard benznidazole as trypanocidal agents. In particular, compounds **52** and **60** are both low nanomolar Cz inhibitors and one-digit nanomolar inhibitors for CatL. Compound **57** had no affinity for any of the six CPs reported herein, which excluded the possibility that its mechanism of action is similar to compound **52** and **60**. Physiochemical properties (logP, MM, TPSA, LogS) play an important role in drug design. As well, for potential trypanocidal agents, which had been designed as protozoan cysteine proteases inhibitors, physicochemical properties can influence their outcome. Therefore, we have included TPSA, calculated logP (ilogP), and LogS (Ali_LogS) in this discussion (Figs 12, 13 and 14) [35].

Table 2. Biological data for trypanocidal activity (EC_{50}), cytotoxicity (CC_{50}), and selective index (SI) for the series of dipeptidyl nitriles.

Compounds	EC_{50} (μM)	CC_{50} (μM)	SI
Benznidazole	4.4 ± 0.47	> 100	> 23
9	72 ± 5.7	> 100	> 1.4
10	67.6 ± 8.22	> 100	> 1.5
12	32.7 ± 3.86	> 100	> 3.1
15	64.7 ± 4.32	73.6 ± 8.74	1.14
16	47.3 ± 3.26	> 100	> 2.1
50	63.3 ± 5.74	83.1 ± 6.85	1.31
51	8.6 ± 0.53	42.3 ± 3.94	4.9
52	4.1 ± 0.47	97.9 ± 6.52	24
53	26 ± 2.6	> 100	> 3.8
54	15.8 ± 1.43	44.7 ± 5.24	2.83
57	4.3 ± 0.32	> 100	> 23
60	4.9 ± 0.45	> 100	> 20
65	70.8 ± 8.79	> 100	> 1.4
66	30.0 ± 2.71	> 100	> 3.3
67	24.4 ± 2.36	> 100	> 4.1
68	16 ± 4.0	> 100	> 6.3
69	30.6 ± 3.11	> 100	> 3.3

Benznidazole was used as a positive control. DMSO was used to dissolve compounds and as a negative control. All data were obtained using at least two independent experiments. Compounds with EC_{50} > 100 μM were considered to be not active, and they are not reported in this Table. Green areas highlight the most potent compounds.

https://doi.org/10.1371/journal.pntd.0007755.t002

In general, the substitution of the P3 or P2 moieties from the prototype compound (**9**) did not result in any increment of potency, except in the case of compound **12** (Fig 12). Modification in P1 strongly modulated the trypanocidal effect. Substitution of Phe for (*S*,*R*)-Thr-O-Bn led to a modest trypanocidal activity. If we consider the physicochemical properties of the whole set of compounds, there is no consistent correlation with their trypanocidal activities. However, when considering discontinuity in small sets of compounds related to their matched molecular pairs (MMP) [36], we observed, in some specific cases, that modulation in compound lipophilicity yields to high trypanocidal potency. For instance, the existence of the molecular pair between compounds **52** (EC_{50} = 4.1 μM; ilogP = 2.3) and **9** (EC_{50} = 71.8 μM; ilogP = 3.2) suggests that the 17.5-fold increase in potency in favor of **52** may be due to its reduced lipophilicity. In addition, single modification in P2 or P1 of compound **9** did not always produce a beneficial effect for the trypanocidal activity. However, considering both modifications [**960**], compound **60** (EC_{50} = 4.9 μM) exhibited a 14.5 times higher trypanocidal potency than compound **9** (EC_{50} = 71.8 μM). Compound **60** displayed activity against the parasite similar to that observed for benznidazole–EC_{50} of 4.4 (Fig 13). Interestingly, the ilogP of 4.1 for **60** was the highest among the entire series and more than one log unit larger than that of compound **52**. Too, compound **57**, which also has ilogP of 4.1, is equipotent to compound **52** whose ilogP is only 2.3! It is noteworthy that compound **57**, exhibiting the same values for TPSA and ilogP as **60** (a high affinity cruzain inhibitor), had no affinity for any of the CPs studied herein. Assumably, compound **57** has a different mode of action than **60**. Furthermore, inhibitor **57** ($CC_{50} \simeq 124.7$ μM) showed the highest selectivity and lowest cytotoxicity in our assays. This guarantees an SI (selective index) ratio of over 20, as well as for compounds **60**

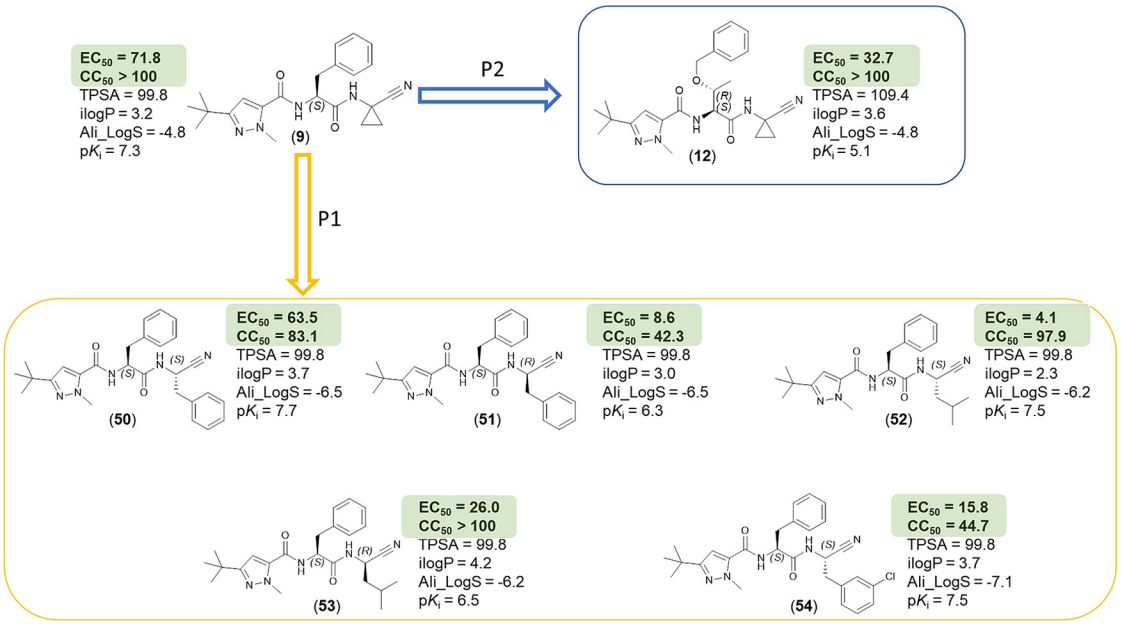

Fig 12. Schematic representation of physicochemical properties and SARs for trypanocidal activity. EC_{50} calculated for amastigote forms of *T. cruzi* (Tuhaluen strain). CC_{50} calculated for the LLCMK2 strain (host cell). Green areas highlight biochemical results. TPSA, ilogP, and Ali_Logs have been calculated with the swissADME online service [35]. pK_i values are referring to Cz inhibition.

https://doi.org/10.1371/journal.pntd.0007755.g012

and **52**, making them appealing targets for further *in vivo* testing against the acute form of Chagas disease [36].

Compounds bearing a leucine moiety in P2 displayed a peculiar behavior (Fig 14). Indeed, the debenzylation of the threonine moiety in P1 led to an increase in potency [**58**→**66**] and

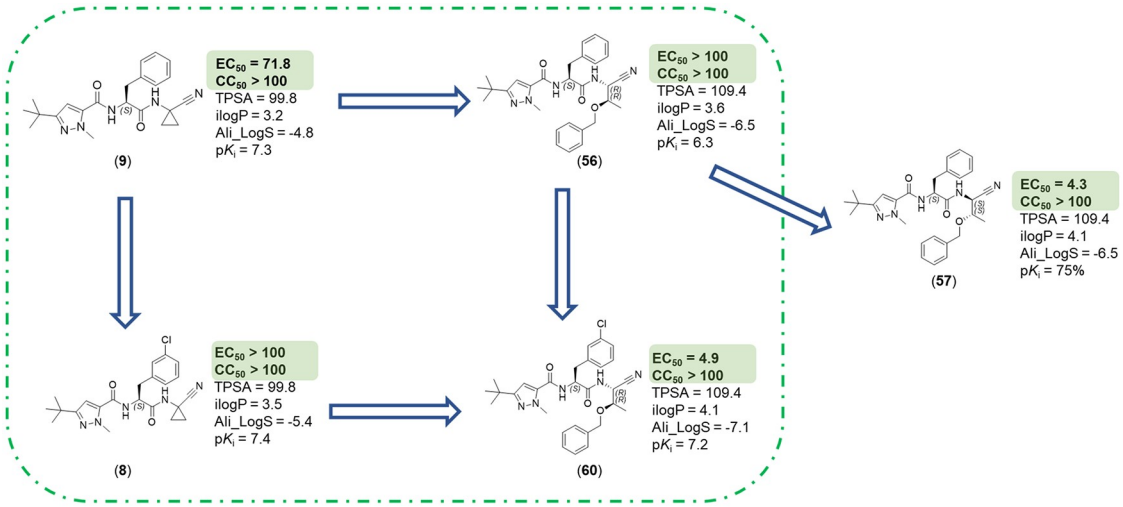

Fig 13. Schematic representation for non-additivity of SARs for trypanocidal activity. EC_{50} calculated for amastigote forms of *T. cruzi* (Tuhaluen strain). CC_{50} calculated for the LLCMK2 strain (host cell). Green areas highlight biochemical results. TPSA, ilogP, and Ali_Logs have been calculated with the swissADME online service [29]. pK_i values are referring to Cz inhibition.

https://doi.org/10.1371/journal.pntd.0007755.g013

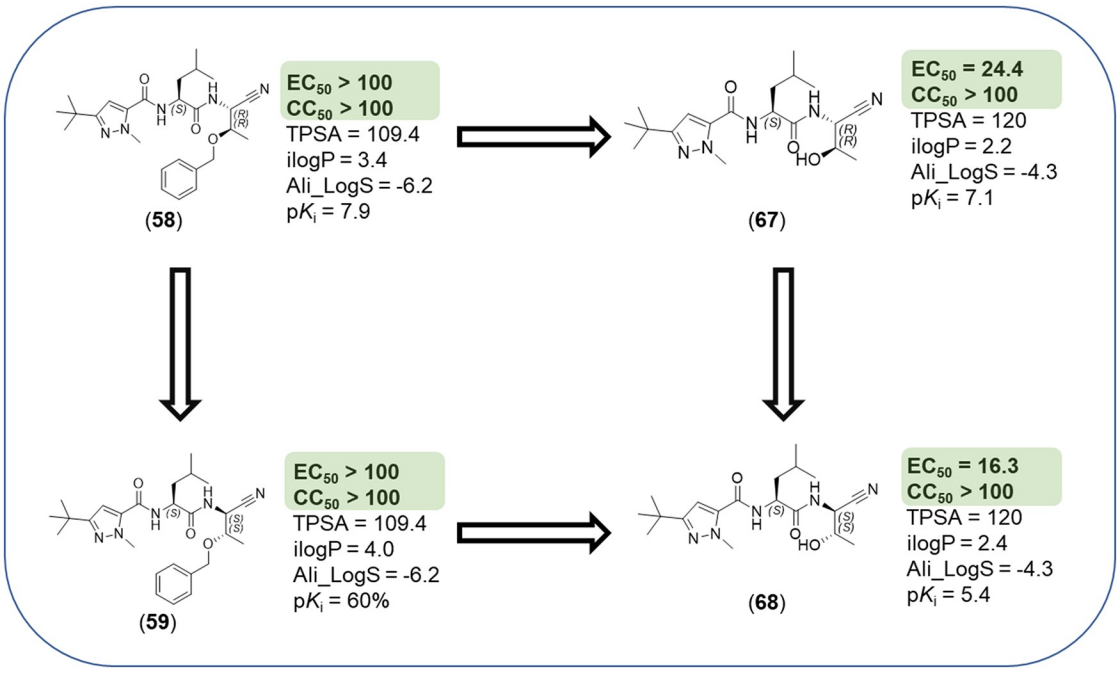

Fig 14. Schematic representation for non-additivity of SARs for compounds 58, 59, 67 and 68. EC_{50} calculated for amastigote forms of *T.cruzi* (Tuhaluen strain). CC_{50} calculated for the LLCMK2 strain (host cell). Green areas highlight biochemical results. TPSA, ilogP, and Ali_Logs have been calculated with the swissADME online service [35]. pK_i values are referring to Cz inhibition.

https://doi.org/10.1371/journal.pntd.0007755.g014

[**59**→**67**]. The trypanocidal potency for this set of compounds seemed not to correlate directly with Cz affinity; but, once again, active compounds had an ilogP value of less than 3.0.

Potential cytotoxicity of inhibitors was assessed with the $LLCMK_2$ cell-based assay, and compounds were evaluated over three days using benznidazole as a control. Cytotoxicity at the highest concentration tested that did not lead to precipitation (250 μM) was low for the majority of test compounds. The most potent inhibitors of the amastigote *T. cruzi* Tulahuen strains (**52, 57** and **60**) showed the same range of cytotoxicity when compared to benznidazole [37]. Based on the data obtained here and supported by previous reports [14,38], the nitrile warhead introduced to target protozoan cysteine protease yields a low cytotoxicity profile. At the same time, our data reflect the difficulty in the translation of biochemical assay results (highlighted here by Cz inhibitors) to trypanocidal action. Since observable in a multitude of systems, this phenomenon is not limited to dipeptidyl nitrile inhibitors, but also known for other compound classes [12,39] targeting the amastigote form of the parasite. The failure of some Cz inhibitors to affect the intracellular amastigote form might be attributed to (i) the interference with the autoproteolytic cruzain activity, (ii) the necessity of crossing two membranes and (iii) the differences of Cz isoforms, *e.g.*, cruzipain 2, with respect to pH stability, substrate specificity, and sensitivity to inhibition by natural and synthetic inhibitors [40]. Hence, even though Cz inhibition is efficient, the parasite would still survive thanks to the action of cruzipain 2. Further insights would be necessary to specify the importance of different cysteine protease forms in the process of target validation for Chagas disease.

Discussion

In this study, we expanded our previous series of dipeptidyl nitrile inhibitors of Cz by leveraging the P1-S1/S1' interaction. Our synthetic route was feasible for a variety of nitrile-based

peptidic inhibitors. In particular, we spotted the Thr-O-Bn moiety in P1 as a malleable building block for the synthesis of such cysteine protease inhibitors. We studied how the P1-S1/S1' interaction can influence affinity and selectivity for two protozoa (Cz and LmCPB) and four mammalians (CatB, CatK, CatL and CatS) CPs. Furthermore, 15 compounds had pEC_{50} values in the range of 4.1–5.4 against the *T. cruzi* amastigote form (pEC_{50} = 5.4 for benznidazole control drug). Three of them (**52, 57** and **60**) are equipotent (pEC_{50} 5.3–5.4) with benznidazole as trypanocidal agents with an SI of over 20, making them attractive targets for further *in vivo* testing against the acute form of Chagas disease. Our work also contributes to the perception of the extrathermodynamic relationship in ligand affinity between Cz and LmCPB, which can be used in LmCPB inhibitor development targeting *Leishmania mexicana*. In this study, we disclosed one strong inhibitor (**14**) of Cz with high selectivity over CatL and two low nanomolar inhibitors of CatL and CatK (compounds **8** and **18**) with more than one log unit selectivity over the other mammalian cysteine proteases. In conclusion, our work contributes to the understanding of subtle drug-target interactions and to the discovery of tailored trypanocidal agents equipotent to benznidazole.

Supporting information

S1 Fig. Extrathermodynamic relationship. Plot of pK_i (Cz) vs. pK_i (LmCPB). A linear trendline fitted points.
(PDF)

S2 Fig. Curves dose-response. Dose curve response for determination of CC_{50} ($LLCMK_2$) and EC_{50} (*T. cruzi* Tulahuen) for all compounds.
(PDF)

S3 Fig. Characterization of final compounds. ^{1}H, ^{13}C NMR spectra and HPLC reports for final compounds.
(PDF)

S1 Table. Biological data for trypanocidal activity. Number identification, Nequimed number, biological data for trypanocidal activity (EC_{50}) and citotoxicity (CC_{50}).
(PDF)

Author Contributions

Conceptualization: Lorenzo Cianni, Jürgen Bajorath, Stefan Laufer, Michael Gütschow, Carlos A. Montanari.

Data curation: Lorenzo Cianni, Carina Lemke, Erik Gilberg, Christian Feldmann, Daiane Y. Tezuka, Carla D. Lopes, Jürgen Bajorath, Andrei Leitão, Michael Gütschow, Carlos A. Montanari.

Formal analysis: Lorenzo Cianni, Carina Lemke, Fabiana Rosini, Daiane Y. Tezuka.

Funding acquisition: Sérgio de Albuquerque, Jürgen Bajorath, Stefan Laufer, Michael Gütschow.

Investigation: Lorenzo Cianni, Carina Lemke, Erik Gilberg, Christian Feldmann, Fabiana Rosini, Fernanda dos Reis Rocho, Jean F. R. Ribeiro, Daiane Y. Tezuka, Carla D. Lopes.

Methodology: Lorenzo Cianni, Carina Lemke, Erik Gilberg, Christian Feldmann, Fabiana Rosini, Fernanda dos Reis Rocho, Jean F. R. Ribeiro, Daiane Y. Tezuka, Carla D. Lopes.

Project administration: Lorenzo Cianni, Stefan Laufer, Michael Gütschow, Carlos A. Montanari.

Resources: Sérgio de Albuquerque, Jürgen Bajorath, Michael Gütschow, Carlos A. Montanari.

Supervision: Lorenzo Cianni, Carla D. Lopes, Sérgio de Albuquerque, Stefan Laufer, Andrei Leitão, Carlos A. Montanari.

Validation: Sérgio de Albuquerque.

Visualization: Fernanda dos Reis Rocho, Sérgio de Albuquerque, Jürgen Bajorath, Stefan Laufer, Andrei Leitão, Michael Gütschow, Carlos A. Montanari.

Writing – original draft: Lorenzo Cianni.

Writing – review & editing: Lorenzo Cianni, Carina Lemke, Erik Gilberg, Christian Feldmann, Daiane Y. Tezuka, Carla D. Lopes, Jürgen Bajorath, Stefan Laufer, Andrei Leitão, Michael Gütschow, Carlos A. Montanari.

References

1. WHO | What is Chagas disease? In: WHO [Internet]. [cited 22 Oct 2019]. http://www.who.int/chagas/disease/en/
2. Prata A. Clinical and epidemiological aspects of Chagas disease. Lancet Infect Dis. 2001; 1: 92–100. https://doi.org/10.1016/S1473-3099(01)00065-2 PMID: 11871482
3. Coura JR, Viñas PA. Chagas disease: a new worldwide challenge. Nature. 2010; 465: S6–S7. https://doi.org/10.1038/nature09221 PMID: 20571554
4. Castro JA, deMecca MM, Bartel LC. Toxic Side Effects of Drugs Used to Treat Chagas' Disease (American Trypanosomiasis). Hum Exp Toxicol. 2006; 25: 471–479. https://doi.org/10.1191/0960327106het653oa PMID: 16937919
5. Urbina JA. Specific chemotherapy of Chagas disease: relevance, current limitations and new approaches. Acta Trop. 2010; 115: 55–68. https://doi.org/10.1016/j.actatropica.2009.10.023 PMID: 19900395
6. Gillmor SA, Craik CS, Fletterick RJ. Structural determinants of specificity in the cysteine protease cruzain. Protein Sci. 1997; 6: 1603–1611. https://doi.org/10.1002/pro.5560060801 PMID: 9260273
7. Cazzulo, JJ. Cruzipain. in Handbook of Proteolytic Enzymes, 3rd. Ed. (J. Rawlings, Ed.). Chapter 437, 1909–1914, 2012, Elsevier, U.K.
8. Engel JC, Doyle PS, Hsieh I, McKerrow JH. Cysteine protease inhibitors cure an experimental Trypanosoma cruzi infection. J Exp Med. 1998; 188: 725–734. https://doi.org/10.1084/jem.188.4.725 PMID: 9705954
9. Sajid M, Robertson SA, Brinen LS, McKerrow JH. Cruzain : the path from target validation to the clinic. Adv Exp Med Biol. 2011; 712: 100–115. https://doi.org/10.1007/978-1-4419-8414-2_7 PMID: 21660661
10. Urbina JA, Docampo R. Specific chemotherapy of Chagas disease: controversies and advances. Trends Parasitol. 2003; 19: 495–501. https://doi.org/10.1016/j.pt.2003.09.001 PMID: 14580960
11. K777 (Chagas) | DNDi. In: Drugs for Neglected Diseases initiative (DNDi) [Internet]. 2 Feb 2011 [cited 17 Jul 2019]. https://www.dndi.org/diseases-projects/portfolio/completed-projects/k777/
12. Cianni L, Feldmann CW, Gilberg E, Gütschow M, Juliano L, Leitão A, et al. Can Cysteine Protease Cross-Class Inhibitors Achieve Selectivity? J Med Chem. 2019; acs.jmedchem.9b00683. https://doi.org/10.1021/acs.jmedchem.9b00683 PMID: 31361135
13. Ndao M, Beaulieu C, Black WC, Isabel E, Vasquez-Camargo F, Nath-Chowdhury M, et al. Reversible Cysteine Protease Inhibitors Show Promise for a Chagas Disease Cure. Antimicrob Agents Chemother. 2014; 58: 1167–1178. https://doi.org/10.1128/AAC.01855-13 PMID: 24323474
14. Avelar LAA, Camilo CD, de Albuquerque S, Fernandes WB, Gonçalez C, Kenny PW, et al. Molecular Design, Synthesis and Trypanocidal Activity of Dipeptidyl Nitriles as Cruzain Inhibitors. Pollastri MP, editor. PLoS Negl Trop Dis. 2015; 9: e0003916. https://doi.org/10.1371/journal.pntd.0003916 PMID: 26173110
15. Cianni L, Sartori G, Rosini F, De DV, Pires G, Lopes BR, et al. Leveraging the cruzain S3 subsite to increase affinity for reversible covalent inhibitors. Bioorganic Chem. 2018; 79: 285–292. https://doi.org/10.1016/j.bioorg.2018.04.006 PMID: 29783099

16. Kramer L, Turk D, Turk B. The Future of Cysteine Cathepsins in Disease Management. Trends Pharmacol Sci. 2017; 38: 873–898. https://doi.org/10.1016/j.tips.2017.06.003 PMID: 28668224

17. Chemical Computing Group Inc. Molecular Operating Environment (MOE). Montreal, Quebec, Canada;

18. Mertens MD, Schmitz J, Horn M, Furtmann N, Bajorath J, Mareš M, et al. A Coumarin-Labeled Vinyl Sulfone as Tripeptidomimetic Activity-Based Probe for Cysteine Cathepsins. ChemBioChem. 2014; 15: 955–959. https://doi.org/10.1002/cbic.201300806 PMID: 24648212

19. Frizler M, Lohr F, Lülsdorff M, Gütschow M. Facing the gem-Dialkyl Effect in Enzyme Inhibitor Design: Preparation of Homocycloleucine-Based Azadipeptide Nitriles. Chem—Eur J. 2011; 17: 11419–11423. https://doi.org/10.1002/chem.201101350 PMID: 21898616

20. Schmitz J, Gilberg E, Löser R, Bajorath J, Bartz U, Gütschow M. Cathepsin B: Active site mapping with peptidic substrates and inhibitors. Bioorg Med Chem. 2019; 27: 1–15. https://doi.org/10.1016/j.bmc.2018.10.017 PMID: 30473362

21. Schmitz J, Beckmann A-M, Dudic A, Li T, Sellier R, Bartz U, et al. 3-Cyano-3-aza-β-amino Acid Derivatives as Inhibitors of Human Cysteine Cathepsins. ACS Med Chem Lett. 2014; 5: 1076–1081. https://doi.org/10.1021/ml500238q PMID: 25313316

22. McGrath ME, Eakin AE, Engel JC, McKerrow JH, Craik CS, Fletterick RJ. The crystal structure of cruzain: a therapeutic target for Chagas' disease. J Mol Biol. 1995; 247: 251–259. https://doi.org/10.1006/jmbi.1994.0137 PMID: 7707373

23. Brinen LS, Hansell E, Cheng J, Roush WR, McKerrow JH, Fletterick RJ. A target within the target: probing cruzain's P1′ site to define structural determinants for the Chagas' disease protease. Structure. 2000; 8: 831–840. https://doi.org/10.1016/s0969-2126(00)00173-8 PMID: 10997902

24. Frizler M, Stirnberg M, Sisay M, Gutschow M. Development of Nitrile-Based Peptidic Inhibitors of Cysteine Cathepsins. Curr Top Med Chem. 2010; 10: 294–322. https://doi.org/10.2174/156802610790725452 PMID: 20166952

25. Beaulieu C, Isabel E, Fortier A, Massé F, Mellon C, Méthot N, et al. Identification of potent and reversible cruzipain inhibitors for the treatment of Chagas disease. Bioorg Med Chem Lett. 2010; 20: 7444–7449. https://doi.org/10.1016/j.bmcl.2010.10.015 PMID: 21041084

26. Asaad N, Bethel PA, Coulson MD, Dawson JE, Ford SJ, Gerhardt S, et al. Dipeptidyl nitrile inhibitors of Cathepsin L. Bioorg Med Chem Lett. 2009; 19: 4280–4283. https://doi.org/10.1016/j.bmcl.2009.05.071 PMID: 19515558

27. Wright JA, Yu J, Spencer JB. Sequential removal of the benzyl-type protecting groups PMB and NAP by oxidative cleavage using CAN and DDQ. Tetrahedron Lett. 2001; 42: 4033–4036. https://doi.org/10.1016/S0040-4039(01)00563-9

28. Montanari ML, Beezer AE, Montanari CA, Piló-Veloso D. QSAR based on biological microcalorimetry. J Med Chem. 2000; 43: 3448–3452. https://doi.org/10.1021/jm990427k PMID: 10978193

29. Núñez S, Venhorst J, Kruse CG. Target-drug interactions: first principles and their application to drug discovery. Drug Discov Today. 2012; 17: 10–22. https://doi.org/10.1016/j.drudis.2011.06.013 PMID: 21777691

30. Geschwindner S, Ulander J, Johansson P. Ligand Binding Thermodynamics in Drug Discovery: Still a Hot Tip? J Med Chem. 2015; 58: 6321–6335. https://doi.org/10.1021/jm501511f PMID: 25915439

31. Khakhel' OA, Romashko TP. Extrathermodynamics: Varieties of Compensation Effect. J Phys Chem A. 2016; 120: 2035–2040. https://doi.org/10.1021/acs.jpca.6b00493 PMID: 26949977

32. Silva DG, Ribeiro JFR, De Vita D, Cianni L, Franco CH, Freitas-Junior LH, et al. A comparative study of warheads for design of cysteine protease inhibitors. Bioorg Med Chem Lett. 2017; 27: 5031–5035. https://doi.org/10.1016/j.bmcl.2017.10.002 PMID: 29054358

33. Schmitz J, Li T, Bartz U, Gütschow M. Cathepsin B Inhibitors: Combining Dipeptide Nitriles with an Occluding Loop Recognition Element by Click Chemistry. ACS Med Chem Lett. 2016; 7: 211–216. https://doi.org/10.1021/acsmedchemlett.5b00474 PMID: 26985300

34. Kramer C, Fuchs JE, Liedl KR. Strong Nonadditivity as a Key Structure–Activity Relationship Feature: Distinguishing Structural Changes from Assay Artifacts. J Chem Inf Model. 2015; 55: 483–494. https://doi.org/10.1021/acs.jcim.5b00018 PMID: 25760829

35. Daina A, Michielin O, Zoete V. SwissADME: a free web tool to evaluate pharmacokinetics, drug-likeness and medicinal chemistry friendliness of small molecules. Sci Rep. 2017; 7: 42717. https://doi.org/10.1038/srep42717 PMID: 28256516

36. Tyrchan C, Evertsson E. Matched molecular pair analysis in short: algorithms, applications and limitations. Comp Struct Biotech J. 2017; 15: 86–90. https://doi.org/10.1016/j.csbj.2016.12.003 PMID: 28066532

37. Chatelain E. Chagas Disease Drug Discovery: Toward a New Era. J Biomol Screen. 2015; 20: 22–35. https://doi.org/10.1177/1087057114550585 PMID: 25245987

38. Gomes JC, Cianni L, Ribeiro J, dos Reis Rocho F, da Costa Martins Silva S, Batista PHJ, et al. Synthesis and structure-activity relationship of nitrile-based cruzain inhibitors incorporating a trifluoroethylamine-based P2 amide replacement. Bioorg Med Chem. 2019; 27: 115083. https://doi.org/10.1016/j.bmc.2019.115083 PMID: 31561938

39. Boudreau PD, Miller BW, McCall L-I, Almaliti J, Reher R, Hirata K, et al. Design of Gallinamide A Analogs as Potent Inhibitors of the Cysteine Proteases Human Cathepsin L and *Trypanosoma cruzi* Cruzain. J Med Chem. 2019; 62: 9026–9044. https://doi.org/10.1021/acs.jmedchem.9b00294 PMID: 31539239

40. Lima APCA, dos Reis FCG, Serveau C, Lalmanach G, Juliano L, Ménard R, et al. Cysteine protease isoforms from Trypanosoma cruzi, cruzipain 2 and cruzain, present different substrate preference and susceptibility to inhibitors. Mol Biochem Parasitol. 2001; 114: 41–52. https://doi.org/10.1016/s0166-6851(01)00236-5 PMID: 11356512